Chemical Studies on Glycoconjugates in Lipoteichoic Acid Fraction of *Enterococcus hirae* ATCC 9790 in Relation to Its Immunobiological Activity

Doctoral Dissertation

by

Masahito Hashimoto

Osaka University

1997

Contents

ABBREVIATIONS

acylGro, acylglycerol

$acyl_2$Gro, 1,2-di-*O*-acylglycerol

BSA, bovine serum albumin

COSY, correlation spectroscopy

DEPT, distortionless enhancement by polarization transfer

DMSO, dimethyl sulfoxide

DNase, deoxyribonuclease

DQF, double quantum filter

ELISA, enzyme-linked immunosorbent assay

ESI, electrospray ionization

FAB, fast atom bombardment

FID, flame ionization detector

GC, gas chromatography

Glc, glucose

Glc_nGro, oligoglucosylglycerol

Gro, glycerol

Hex, hexose

HMBC, heteronuclear multiple bond connectivity

HMQC, homonuclear multi quantum coherence

HPLC, high performance liquid chromatography

ICP, inductively coupled plasma

IL, interleukin

Man, mannose

MALDI, matrix assisted laser desorption ionization

MS, mass spectrometry

NMR, nuclear magnetic resonance

NOE, nuclear Overhauser effect

NOESY, nuclear Overhauser effect spectroscopy

PAGE, polyacrylamide gel electrophoresis

PBS, phosphate-buffered saline

RNase, ribonuclease

SDS, sodium dodecyl sulfate

TFA, trifluoroacetic acid

TLC, thin layer chromatography

TNF, tumor necrosis factor

TOCSY, total correlation spectroscopy

TOF, time of flight

I. Introduction

It has been reported that various glycoconjugates which modulate host defence functions are located in the surface layers of bacterial cells (Table 1-1) (*1*). Lipopolysaccharide (LPS [2]) which is an outer membrane component of Gram-negative bacteria triggers a release of TNF-α (*3*), IL-1β (*4*), IL-6 (*5*), IL-12 (*6*), and nitrite (*7*) and induces a tumoricidal activity in macrophage (*8*). Peptidoglycan (PG [*9*]) which is a cell wall component of most bacteria exerts LPS-like properties (*10*) and an adjuvant effect on immune responses (*11*, *12*). These glycoconjugates have been well investigated and the minimum structures responsible for their biological activity have already been chemically defined. Lipid A, the glycolipid part in LPS, is responsible for most of the endotoxic activity (*13*), and muramyl dipeptide, N-acetylmuramyl-L-alanyl-D-isoglutamate, is responsible for the adjuvant effects of PG (*14*).

Lipoteichoic acid (LTA) is a macroamphiphile distributed on the cell surface of Gram-positive bacteria (*15*). LTA is usually isolated by hot phenol-water extraction followed by hydrophobic interaction chromatography or ion-exchange chromatography (*16*). LTA is not a homogeneous compound but a mixture of congeners with a wide molecular weight range. The basic structures of several LTAs and their heterogeneity were proposed by Fischer (*15*). According to him, enterococcal and streptococcal LTAs, for example, are composed of a glycolipid anchor and a 1,3-linked poly(glycerophosphate) chain with oligoglucosyl or D-alanyl substitutions at the 2-positions of the glycerols (Figure 1-1).

In the 1980s, distinct immunobiological activities of enterococcal and streptococcal LTAs were described. Yamamoto *et al.* (*17, 18*) and Usami *et al.* (*19, 20*) reported that LTA,

Table 1-1. Biological response modifiers (BRMs) in bacterial cell surfaces.

BRM	Occurrence	Essential structure for activities	Biological activities
Lipopolysaccharide (LPS)	Outer membrane of Gram-negative bacteria	Lipid A	Cytokine-inducing activity Antitumor activity
Peptidoglycan (PG)	Cell wall of most of bacteria	Muramyl dipeptide	Cytokine-inducing activity Antitumor activity Adjuvant effects
Lipoteichoic acid (LTA)	Cell surface of Gram-positive bacteria	?	Cytokine-inducing activity Antitumor activity

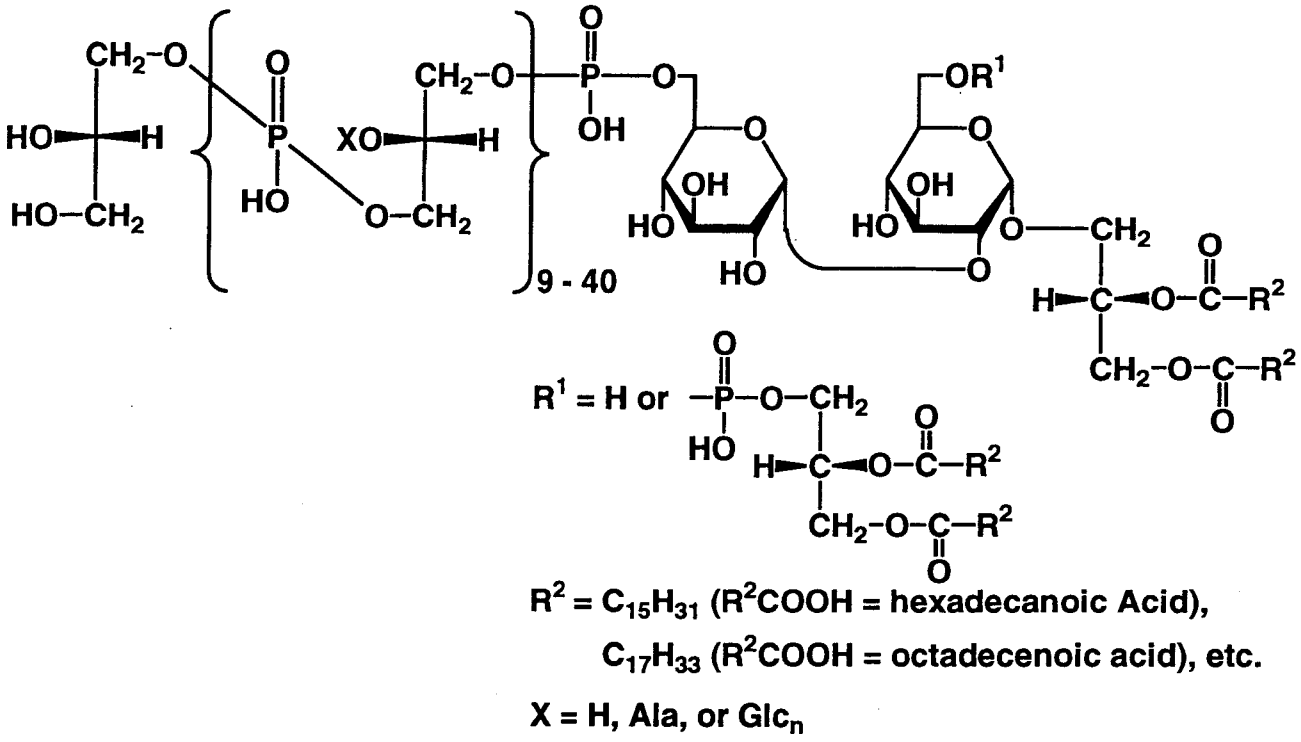

Figure 1-1. Structures proposed for enterococcal and streptococcal LTAs.

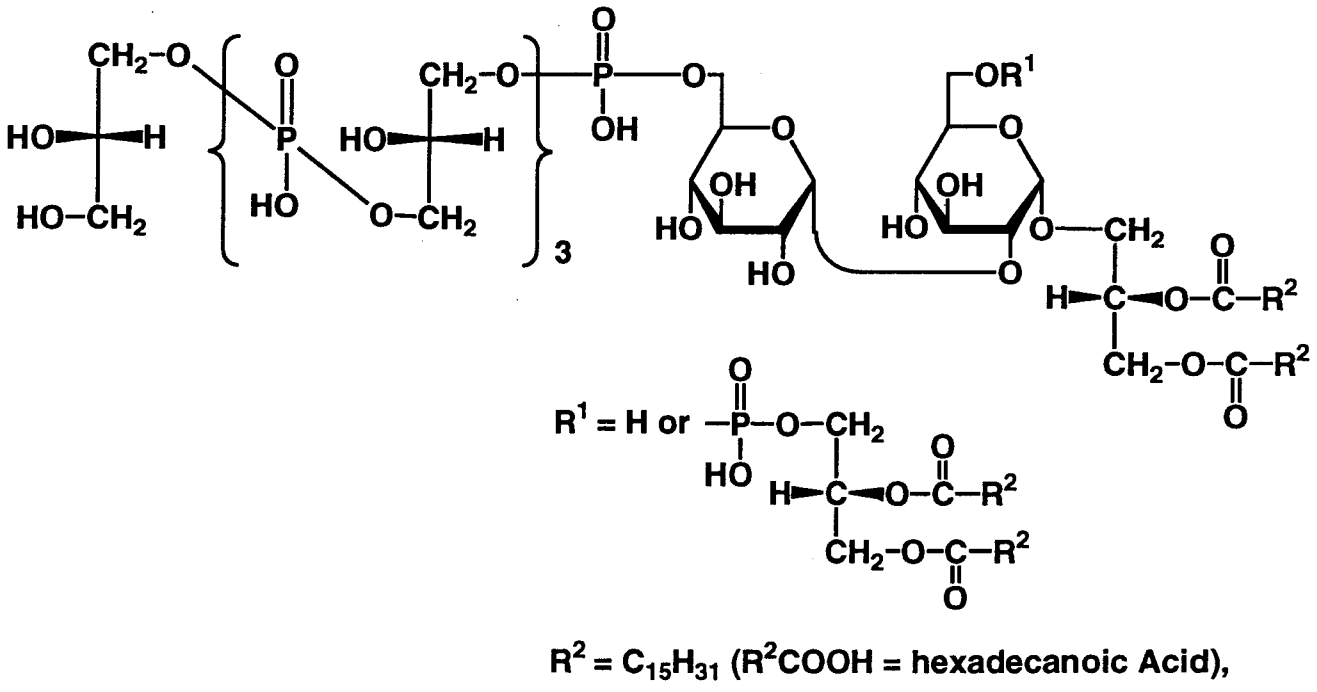

Figure 1-2. Compounds synthesized according to the fundamental structures proposed for LTAs from *E. hirae* and *S. pyogenes*.

prepared from *Streptococcus pyogenes*, induced TNF-α and possessed an antitumor activity. Tsutsui *et al.* (*21*) reported that LTA, prepared from *Enterococcus hirae* ATCC 9790, induced TNF-α and IL-1. Bhakdi *et al.* (*22*) reported that LTAs from several enterococci and streptococci had ability to stimulate the production of TNF-α, IL-1β, and IL-6.

Tsutsui *et al.* (*21*) also described that the hydrochloric acid-treated LTA, in which the poly(glycerophosphate) was partially hydrolyzed, still retained the cytokine-inducing activities. On the other hand, the alkali-treated LTA lacking the all acyl moieties lost the activities. These results suggested that the whole structure of LTA was not necessary for the activity, but the glycolipid part with acyl moieties was essential. To find the essential structure in LTA responsible for its cytokine-inducing activity, Fukase *et al.* (*23*, *24*) synthesized the proposed fundamental structures of LTAs from *E. hirae* and *S. pyogenes* (Figure 1-2). Surprisingly, however, neither cytokine-inducing activity nor antitumor activity was observed in the synthetic products (*25*). The structure of the synthetic compounds had several obvious differences from those proposed for natural LTA: (i) the glycolipid anchor in natural LTA contains unsaturated fatty acids, whereas the synthetic ones contain only saturated acids; (ii) the poly(glycerophosphate) in natural LTA was assumed to have between repeating units 9 and 40 (*26*), whereas that of the synthetic ones contains only 4 units; (iii) the synthetic poly(glycerophosphate) part had no substituents in contrast to the high glucosyl and appreciable alanyl substitution described for natural LTA (*15*). The lack of activity in the synthetic compounds may thus be attributable to either of the following two possibilities: (i) some or all of the structural differences between natural LTA and the synthetic compounds are essential for the activity of LTA; (ii) unknown components present in LTA are responsible for the observed activity. Suda *et al.* (*27*) have recently succeeded in separating the LTA fraction from *E. hirae* ATCC 9790 into cytokine-inducing minor components and a major but not cytokine-inducing component which amounts to over 90 wt% of the whole LTA fraction; this favors the latter possibility rather than the former. However, the chemical structures of the components were

not elucidated at that time.

In the present study, the author aimed at the structural elucidation of components in the LTA fraction. In Chapter II is described separation of the cytokine-inducing components and major components which lack the activity. The structural analysis of the later inactive component is described in Chapter III. In Chapter IV is dealt with the structural analysis of one of the cytokine-inducing components.

From the result of the present study, the author concluded that the major molecular species, which exhibits the so-called LTA structure proposed by Fischer, is not responsible for the cytokine-inducing activity of the LTA fraction. Rather the activity is caused by the novel minor glycoconjugates, one of which was studied for their fundamental structure.

REFERENCES

1) For a review, see: Kotani, S. (1992) *Adv. Exp. Med. Biol.* **319**, 145-164.

2) Rietschel, E.Th., Brade, L., Lindner, B., and Zähringer, U. (1992) in *Bacterial Endotoxic Lipopolysaccharides Vol. I, Molecular Biochemistry and Cellular Biology* (Morrison, D.C. and Ryan, J.L., eds.), pp. 3-41, CRC Press, Boca Raton.

3) Carswell, E.A., Old, L.J., Kassel, R.L., Green, S., Fiore, N., and Williamson., B. (1975) *Proc. Natr. Acad. Sci. USA* **72**, 3666-3670.

4) Hazuda, D.J., Lee, J.C., and Young, P.R. (1988) *J. Biol. Chem.* **263**, 8473-8479.

5) Tosato, G., Seamon, K.B., Goldman, N.D., Seghal, P.B., May, L.T., Washington, G.C., Jones, K.D., and Pike, S.E. (1988) *Science* **239**, 502-504.

6) Heinzel, F.P., Rerko, R.M., Ling, P., Hakimi, J., and Schoenhaut, D.S. (1994) *Infect. Immun.* **62**, 4244-4249.

7) Stuehr, D.J. and Marletta, M.A. (1987) *Cancer Res.* **47**, 5590-5594.

8) Doe, W.F. and Henson, P.M. (1978) *J. Exp. Med.* **148**, 544-556.

9) Takada, H. and Kotani, S. (1985) in *Immunology of the Bacterial Cell Envelope* (Stewart-Tull, D.E.S. and Davies, M., Eds.) pp. 119-152, John Wiley and Sons, Chichester.

10) Mattsson, E., Verhage, L., Rollof, J., Fleer, A., Verhoef, J., and Dijk, H. (1993) *FEMS Immuol. Med. Microbiol.* **7**, 281-288.

11) Adam, A., Ciorbaru, R., Elloux, F., Petit, J.-F., and Lederer, E. (1974) *Biochem. Biophys. Res. Commun.* **56**, 561-567.

12) Nauciel, C., Fleck, J., Martin, M.P., Mock, M., and Nguyen-Huy, H. (1974) *Eur. J. Immunol.* **4**, 352-356.

13) Galanos, C., Lüderitz, O., Rietschel, E.Th., Westphal, O., Brade, H., Brade, L., Freudenberg, M., Schade, U., Imoto, M., Yoshimura, H., Kusumoto, S., and Shiba, T. (1985) *Eur. J. Biochem.* **148**, 1-5.

14) Kotani, S., Watanabe, Y., Kinoshita, F., Shimono, T., Morisaki, I., Shiba, T., Kusumoto, S., Tarumi, Y., and Ikenaka, K. (1975) *Biken J.* **18**, 105-111.

15) Fischer, W. (1990) in *Glycolipids, Phosphoglycolipids and Sulfoglycolipids* (Kates, M., ed.) pp. 123-234, Plenum Press, New York.

16) Fischer, W., Koch, H.U., and Hass, R. (1983) *Eur. J. Biochem.* **133**, 523-530.

17) Yamamoto, A., Usami, H., Nagamuta, M., Sugawara, Y., Hamada, S., Yamamoto, T., Kato, K., Kokeguchi, S., and Kotani, S. (1985) *Br. J. Cancer* **51**, 739-742.

18) Yamamoto, A., Nagamuta, M., Usami, H., Sugawara, Y., Watanabe, N., Niitsu, Y., and Urushizaki, I. (1985) *Immunol. Lett.* **11**, 83-88.

19) Usami, H., Yamamoto, A., Sugawara, Y., Hamada, S., Yamamoto, T., Kato, K., Kokeguchi, S., Takada, H., and Kotani, S. (1987) *Br. J. Cancer* **56**, 797-799.

20) Usami, H., Yamamoto, A., Yamashita, W., Sugawara, Y., Hamada, S., Yamamoto, T., Kato, K., Kokeguchi, S., Ohokuni, H., and Kotani, S. (1988) *Br. J. Cancer* **57**, 70-73.

21) Tsutsui, O., Kokeguchi, S., Matsumura, T., and Kato, K. (1991) *FEMS Microbiol. Immunol.* **76**, 211-218.

22) Bhakdi, S., Klonisch, T., Nuber, P., and Fischer, W. (1991) *Infect. Immun.* **59**, 4614-4620.

23) Fukase, K., Matsumoto, T., Ito, N., Yoshimura, T., Kotani, S., and Kusumoto, S. (1992) *Bull. Chem. Soc. Jpn.* **65**, 2643-2654.

24) Fukase, K., Yoshimura, T., Kotani, S., and Kusumoto, S. (1994) *Bull. Chem. Soc. Jpn.* **67**, 473-482.

25) Takada, H., Kawabata, Y., Arakaki, R., Kusumoto, S., Fukase, K., Suda, Y., Yoshimura, T., Kokeguchi, S., Kato, K., Komuro, T., Tanaka, N., Saito, M., Yoshida, T., Sato, M., and Kotani, S. (1995) *Infect. Immun.* **63**, 57-65.

26) Leopold, K. and Fischer, W. (1991) *Eur. J. Biochem.* **196**, 475-482.

27) Suda, Y., Tochio, H., Kawano, K., Takada, H., Yoshida, T., Kotani, S., and Kusumoto, S. (1995) *FEMS Immunol. Med. Microbiol.* **12**, 97-112.

II. Separation of the cytokine-inducing components of the lipoteichoic acid fraction

As described in Chapter I, Suda *et al.* have recently succeeded to separate the cytokine-inducing minor components from the LTA fraction of *E. hirae* ATCC 9790 (*1*). They assumed that the components are responsible for the immunobiological activity of the whole LTA fraction. The chemical composition analysis and the SDS-PAGE profiles of the active components revealed that all of them were high-molecular weight glycoconjugates having broad molecular weight ranges (8×10^3-1.7×10^4). Their chemical structures, however, were not determined because of their low contents in the bacterial cells. To elucidate the structure of such complicate molecules, isolation of higher amounts of the components is inevitably required by developing a rapid and efficient method. The major parts of the previous separation procedure were composed of repeated column chromatographies with linear gradients, which were not practical for a large scale fractionation particularly because of a flow rate limitation. Thus, in the present work, an improved method for the separation using batch-wise and stepwise elution has been developed.

MATERIALS AND METHODS

Bacterial Cells

E. hirae ATCC 9790 was grown in 150-liter batches. The growth medium (1-liter)

contained 10 g glucose, 15 g trypticase, 4 g tryptose, 4 g yeast extract, 2 g K_2HPO_4, 5 g KH_2PO_4, 2 g Na_2CO_3, and 2 g NaCl. The bacteria were grown with stirring and slight aeration at 37°C for 6 h using MPF-U200L (L. E. Marubishi Co. Ltd., Japan), harvested by centrifugation, washed three times with PBS, and stored in acetone at 4°C until use. The bacteria were grown totally seven times.

Separation of the cytokine-inducing components

1. Extraction of bacterial cells

The bacterial cells (from one batch of culture) were suspended in 0.1 M acetate buffer (pH 4.5), chloroform, and methanol (500 ml / 500 ml / 1000 ml). The suspension was stirred at room temperature overnight. After centrifugation at 3300 x g for 20 min, the solvent was decanted. The residue was washed twice with methanol and dried *in vacuo* to give delipidated cells in which free, but unbound, lipid were removed. The delipidated cells weighed on the average 0.99 g per 1 liter of the culture.

The delipidated cells (100 g) were milled in a mortar and suspended in 650 ml of 0.1 M acetate buffer (pH 4.5). After addition of 650 ml of 80% phenol (in the same buffer), the suspension was stirred at 65°C for 45 min. After cooling in an ice bath, the aqueous phase was separated by centrifugation at 15000 x g for 20 min. The residual phenolic mixture was suspended in 650 ml of 0.1 M acetate buffer (pH 4.5) and stirred at 65°C for 45 min. After cooling, the aqueous phase was separated by centrifugation. The combined aqueous phase was thoroughly dialyzed against deionized water (prepared by Toray pure LV-308, Toray, Tokyo, Japan) at 4°C for a few days (the all following dialyses in this work were done under similar conditions), concentrated *in vacuo* to about 200 ml with a rotary evaporator, and lyophilized to give a crude extract. The yield was *ca.* 5% from delipidated cells.

All the crude extracts from seven batches were combined. The combined extract (50.0 g) was dissolved in 2.5 liters of 0.1 M acetate buffer containing 5 mM $MgSO_4$ (pH 6.0). After

addition of RNase (450 mg, R-5125, Sigma Chemical Co., St. Louis, MO, USA) and DNase (150 mg, D-5025, Sigma), the mixture was stirred at room temperature for 24 h. The reaction mixture was dialyzed and concentrated *in vacuo* to about 150 ml with a rotary evaporator. After removing the precipitates by centrifugation, the supernatant was lyophilized to give a crude LTA preparation.

2. Fractionation of the crude LTA by Octyl-Sepharose

A solution of the crude LTA (1.0 g) in 200 ml of 0.1 M acetate buffer (pH 4.5) containing 15% 1-propanol was added to 400 ml of Octyl-Sepharose (Pharmacia LKB, Uppsala, Sweden) equilibrated with the same buffer. The mixture was allowed to stand at 4°C for 30 min and filtered. The Octyl-Sepharose was again suspended in 250 ml of the same buffer, allowed to stand at 4°C for 30 min and filtered. This procedure was repeated four more times. The recovered Octyl-Sepharose was treated similarly with the acetate buffer containing 40% 1-propanol (four times) and then with that containing 60% 1-propanol (six times). The filtrates obtained were separately combined, concentrated *in vacuo* to about 100 ml, dialyzed, again concentrated *in vacuo*, and lyophilized to give three fractions, which were designated BOS15 (Batch-wise Octyl-Sepharose eluate with a buffer containing 15% 1-propanol), BOS40, and BOS60, respectively. The yields of the respective fractions were *ca.* 30, 45, and 10% from the crude LTA.

3. Fractionation of the Octyl-Sepharose fractions by ion-exchange membrane

A portion of BOS40 or BOS60 (50 mg) was dissolved in 6 ml of 0.01 M acetate buffer (pH 4.5) containing 35% 1-propanol and applied to an ion-exchange membrane, QMA-Mem Sep 1010 (PerSeptive Biosystems, Framingham, MA, USA), equilibrated with the same buffer. The membrane was washed with 100 ml of the same buffer at 4°C at a flow rate of 3.3 ml/min. The eluate was concentrated *in vacuo* to about 40 ml with a rotary evaporator. The

materials bound to the membrane were then eluted with 100 ml of the buffer containing 35% 1-propanol and 1 M NaCl. The eluate was concentrated. Both eluates were dialyzed separately, concentrated *in vacuo*, and lyophilized to give two fractions, low-anionic and high-anionic fractions which were designated QM-A and QM-I, respectively. Similar procedures were repeated several times and the yield of QM-A and QM-I from BOS40 and BOS60 were almost identical, that of QM-A being in the range of 2-3% and that of QM-I 70-90%, respectively.

4. Further separation of the low-anionic fractions by an Octyl-Sepharose column

The low-anionic fractions (QM-A from BOS40 and QM-A from BOS60) were combined. A part of the combined QM-A (120 mg) was dissolved in 10 ml of 0.1 M acetate buffer (pH 4.5) containing 15% 1-propanol and applied to an Octyl-Sepharose CL-4B column (2.5 x 30 cm) equilibrated with the same buffer. The column was eluted with a linear gradient of 1-propanol (15-60%) at 4°C at a flow rate of 24 ml/h. The fraction of 6 ml was collected and monitored by measuring the phosphorus content. The eluates were divided into five fractions (designated OS-1 to -5), dialyzed, concentrated *in vacuo* with a rotary evaporator, and lyophilized separately. The yields of OS-1 to OS-5 were 8.8, 1.3, 3.9, 47, and 15%, respectively.

OS-4 (42.3 mg) was further purified by an ion-exchange membrane, QMA-Mem Sep 1010, by the same stepwise elution as above to give two fractions, low-anionic fraction (OS-4L) and high-anionic fraction (OS-4H) in the yields of 12 and 58%, respectively.

OS-5 (26.0 mg) was partitioned with 2 ml of chloroform-methanol-water (2/1/3, v/v/v). The aqueous phase was lyophilized to give OS-5W (18% based on OS-5).

Analytical procedures

1. Phosphorus

Phosphorus contents were determined according to the method of Bartlett (2) with a

slight modification. In a test tube (12 x 120 mm), 100 μl of a sample solution, 100 μl of water, 50 μl of concentrated sulfuric acid, and 50 μl of 60% aqueous perchloric acid were mixed and heated in a TAH-2G dry thermo unit (Taitec, Tokyo, Japan) at 200°C for 2 h. After cooling, 100 μl of water and 1.8 ml of 0.5% aqueous ammonium molybdate were added. After vortexing, 20 μl of the reducing reagent (described below) was added. The mixture was vortexed immediately and kept stand for 45 min at room temperature. Then, the absorbance at 675 nm of the solution was measured by a UV-160A UV-visible spectrophotometer (Shimadzu, Kyoto, Japan).

The reducing reagent was prepared as follow: 0.25 g of 1-amino-2-naphthol-4-sulfonic acid, 1 g of sodium sulfite, and 15 g of sodium hydrogensulfite were milled in a mortar and stored in the dark. The mixed reagents were dissolved in water (100 mg/ml) just before use.

2. Hexose

Hexose contents were determined by the anthrone-sulfuric acid method (*3*). In the test tube (12 x 100 mm), 100 μl of a sample solution and 500 μl of an anthrone solution (40 mg/ml in a mixture of water-sulfuric acid [5/19, v/v]) were mixed. After vortexing, the mixture was heated at 100°C for 10 min. After cooling and thorough vortexing, the absorbance at 620 nm of the solution was measured.

Induction and determination of the level of IL-6

IL-6 induction in human peripheral whole-blood cell culture and the determination of its level using ELISA were performed according to the method of Suda *et al.* (*1*) A mixture consisting of a test sample (in 25 μl of saline), 25 μl of heparinized human peripheral whole-blood collected from an adult volunteer, and 75 μl of RPMI 1640 medium (Flow Laboratories, Irvine, Scotland, UK), was incubated in triplicate in a 96-well plastic plate (25850-96, Corning Lab. Sci. Company, Corning, NY, USA) at 37°C in 5% CO_2 for 24 h. The plate was

centrifuged at 300 x g for 2 min. The supernatant was separated and stored at -35°C until use.

Goat anti human IL-6 antiserum (Innogenetics, Twijndrecht, Belgium) diluted to $1/10^3$ in 0.1 M sodium bicarbonate buffer (pH 9.6) (150 µl) was placed in each well of a 96-well ELISA plate (SUMILON MS-8596F, Sumitomo Bakelite Co. Ltd., Tokyo, Japan) and incubated at 4°C overnight. After washing the wells four times with 300 µl of PBS containing 0.05% Tween 20 (PBS-T), 300 µl of 1% BSA in PBS containing 0.1% NaN_3 was placed in each well and incubated at 4°C overnight. After four washes with PBS-T, 20 µl of the supernatant from stimulated whole-blood cell cultures and 80 µl of PBS containing 0.1% BSA and 0.1% NaN_3 was added and incubated at 4°C overnight. After a thorough wash with PBS-T, 100 µl of anti-IL-6 monoclonal antibody conjugated with horseradish peroxidase (Fuji Rebio Co., Tokyo, Japan) was added and the mixture incubated at room temperature for 2 h. After removing the supernatant, 100 µl of a substrate solution consisting of 2,2-azinobis-(3-ethylbenzothiazoline-6-sulfonic acid) diammonium salt (60 mg) and 35% hydrogen peroxide (60 µl) in 0.1 M sodium dihydrogenphosphate (100 ml) was added. After incubation at room temperature for 30 min, 100 µl of 1 M sulfuric acid was added to terminate the enzymatic reaction. The absorbance of each well was measured using an ImmunoMini NJ-2300 microplate reader (InterMed, Tokyo, Japan) at 414 and 492 nm simultaneously, the latter being used as a reference. The IL-6 level (pg/ml) in the supernatant was calibrated by recombinant human IL-6 (a gift from Prof. T. Kishimoto) (*4, 5*).

Both the dose of test samples and the level of induced cytokines were expressed as the final concentration in above mixture (µg/ml and pg/ml, respectively). Among peripheral whole-blood samples from different donors, small but discernible differences were evident regarding the susceptibility to cytokine induction by test samples. Therefore, all of the data presented in each Figure were obtained from the same day assay with a whole-blood sample drawn from one donor as one set of experiment, and so are completely comparable. An LPS specimen prepared by Westphal method from *E. coli* O111:B4 (Sigma) was used as a positive

control to check the response of whole-blood cell cultures to IL-6 induction by test materials throughout the present study. To compare the induction levels between different assays, the levels were normalized by conversion to the corresponding amount of the LPS which triggered to release the same level of IL-6.

Limulus assay

Limulus activity of a sample was measured by means of the Endospecy Test® (Seikagaku Corporation, Tokyo, Japan) using an LPS specimen from *E. coli* O111:B4 (Sigma) as a reference standard. A solution of a test sample in distilled water (20 μl) was mixed with the reagent in the Endospecy ES-200 set (30 μl) and incubated in duplicate in a 96-well plastic plate (Toxipet plate 96F, Seikagaku Corporation) at 37°C for 30 min. Sodium nitrate (75 μl, 0.04% in 0.48 M hydrochloric acid), 75 μl of 0.3% ammonium sulfate, and 75 μl of 0.07% N-1-naphthylethylenediamine dichloride were added successively. The absorbance at 545 nm of each well was measured using a micro plate reader. The levels of *Limulus* activity were evaluated in terms of the amount of the LPS which gave the same absorbance value.

Miscellaneous

Contamination of test materials and instruments with extraneous bacterial endotoxins were carefully prevented. For example, endotoxin-free water purchased from Otsuka (Tokyo, Japan) or prepared by a combination of Toray Pure LV-308 (Toray) and GSL-200 (Advantec, Tokyo, Japan) was used throughout the study.

RESULTS AND DISCUSSION

The separation procedure for the cytokine-inducing components in the previous work

Scheme 2-1. The previous separation procedure for the cytokine-inducing components from *E. hirae* bacteria by Suda *et al.* (*1*).

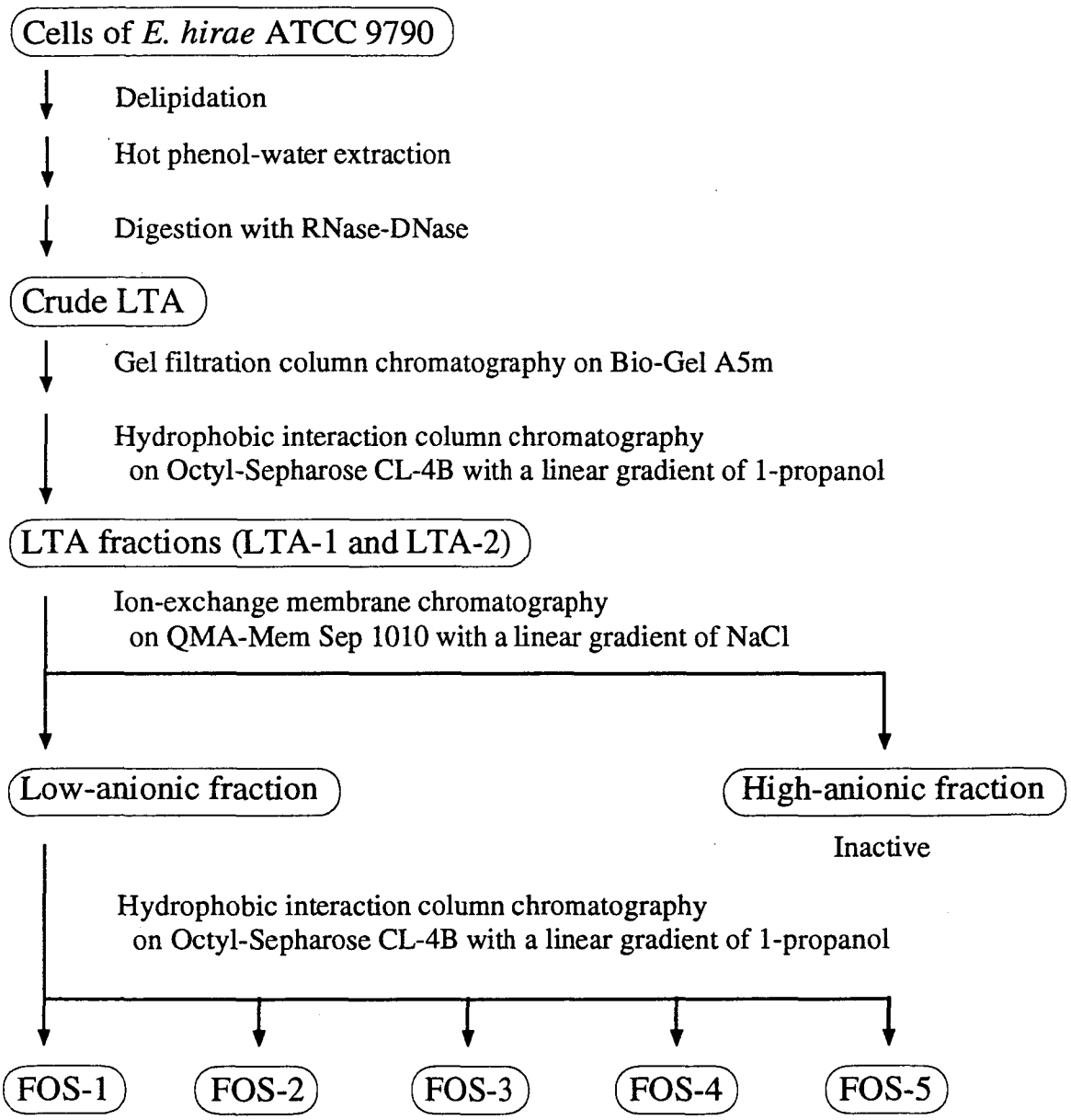

Scheme 2-2. The improved separation procedure for the cytokine-inducing fractions from *E. hirae* cells.

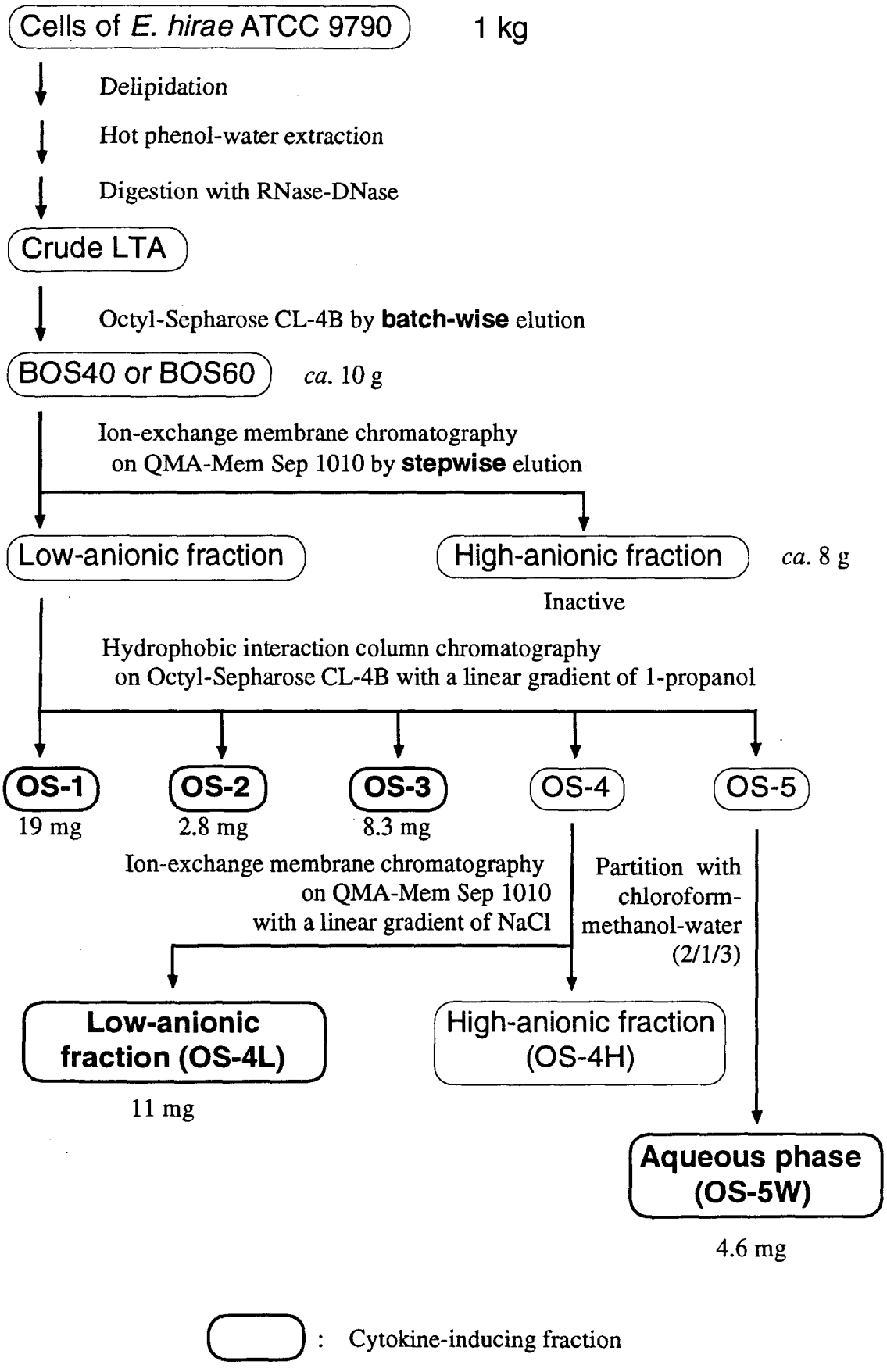

by Suda *et al.* (*1*) is outlined in Scheme 2-1. The bacterial cells were delipidated and extracted with hot phenol-water, and the crude extract was digested with DNase and RNase and dialyzed to give a crude LTA. The isolation of LTA fractions from the crude LTA was performed by two successive chromatographic separations: (i) gel filtration column chromatography on Bio-Gel A5m (Bio Rad Lab., Inc, Hercules, CA, USA) to remove the digested fragments of DNA and RNA; (ii) hydrophobic interaction column chromatography on Octyl-Sepharose CL-4B with a liner gradient of 1-propanol (15-60%) to give two LTA fractions, LTA-1 and LTA-2, in the yield of 30-50% and 7-14%, respectively. Further fractionation of the LTA fraction was performed by ion-exchange membrane chromatography on QMA-Mem Sep 1010 with a liner gradient of NaCl (0-1 M) to give a low-anionic cytokine-inducing fraction and a high-anionic non-inducing fraction. Further separation of the low-anionic fraction was performed by hydrophobic interaction column chromatography on Octyl-Sepharose CL-4B with a liner gradient of 1-propanol (15-60%) to give five components. Good separation was achieved by this separation procedure in small scale experiments. This procedure, however, was not practical for large scale fractionation because of the time-consuming separation in column chromatographies owing to the flow rate limitation. Elution with a linear gradient was also to be improved. Thus, in the study, batch-wise and stepwise elution were employed to achieve rapid and efficient separation (outlined in Scheme 2-2.).

Suda *et at.* showed that the LTAs were adsorbed on Octyl-Sepharose equilibrated in 15% 1-propanol, but the digested fragments of DNA and RNA in the crude LTA were not adsorbed. This proved that nucleic acid fragments are readily separable from the LTAs by batch-wise elution on Octyl-Sepharose: the gel filtration chromatography employed by their work to remove nucleic acid fragments can be omitted. In the present study, crude LTA was directly subjected to batch-wise separation on Octyl-Sepharose. Washing 0.1 M acetate buffer containing 15% 1-propanol afforded the passing through fraction (BOS15). The Octyl-Sepharose was then successively washed with 0.1 M acetate buffer containing 40 and 60% 1-

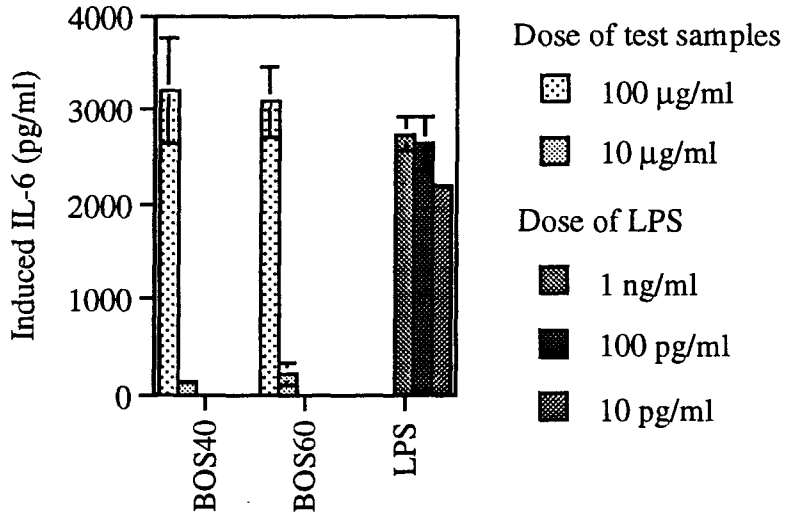

Figure 2-1. IL-6 inducing activity of BOS40 and BOS60. Data are means ±SD of two experiments. The blood donor was JY.

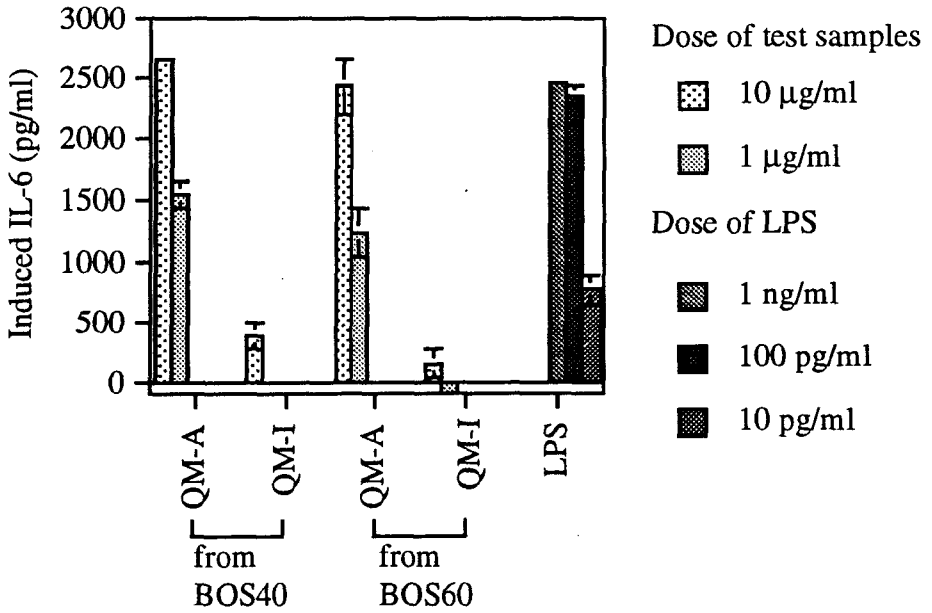

Figure 2-2. IL-6 inducing activity of QM-A and QM-I from BOS40 and BOS60. Data are means ±SD of two experiments. The blood donor was MH.

Table 2-1. The average yields of QM-A and QM-I separated from BOS40 and BOS60, and LTA-1 and LTA-2 by ion-exchange membrane chromatography on QMA-Mem Sep 1010.

	QM-A (%)	QM-I (%)
BOS40	2.6	88
BOS60	3.2	71
LTA-1[a)]	1.4	84
LTA-2[a)]	3.4	72

a) The separation was performed with a linear gradient of NaCl.

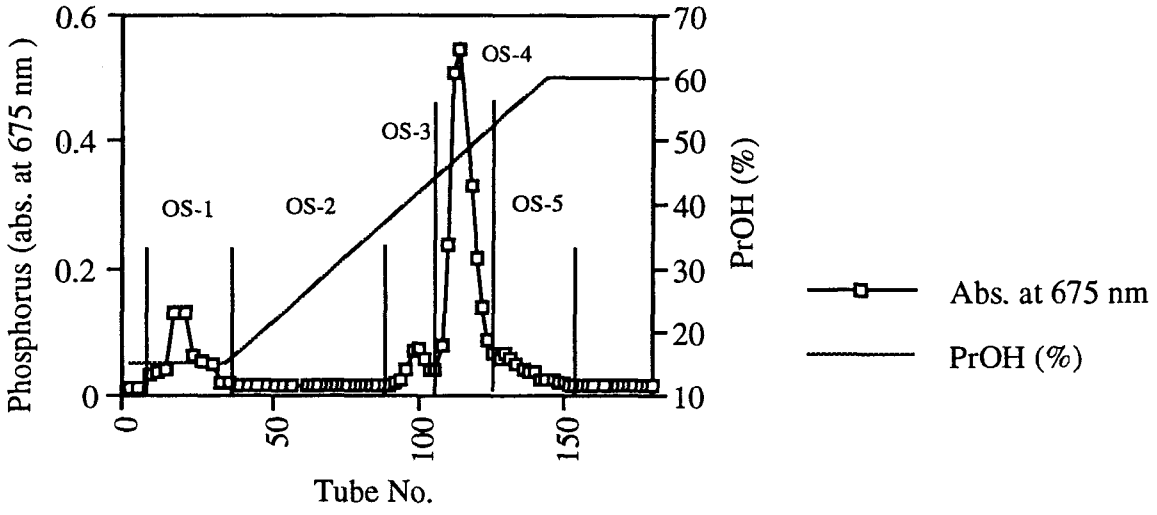

Figure 2-3. The elution profile of the combined QM-A on Octyl-Sepharose CL-4B.

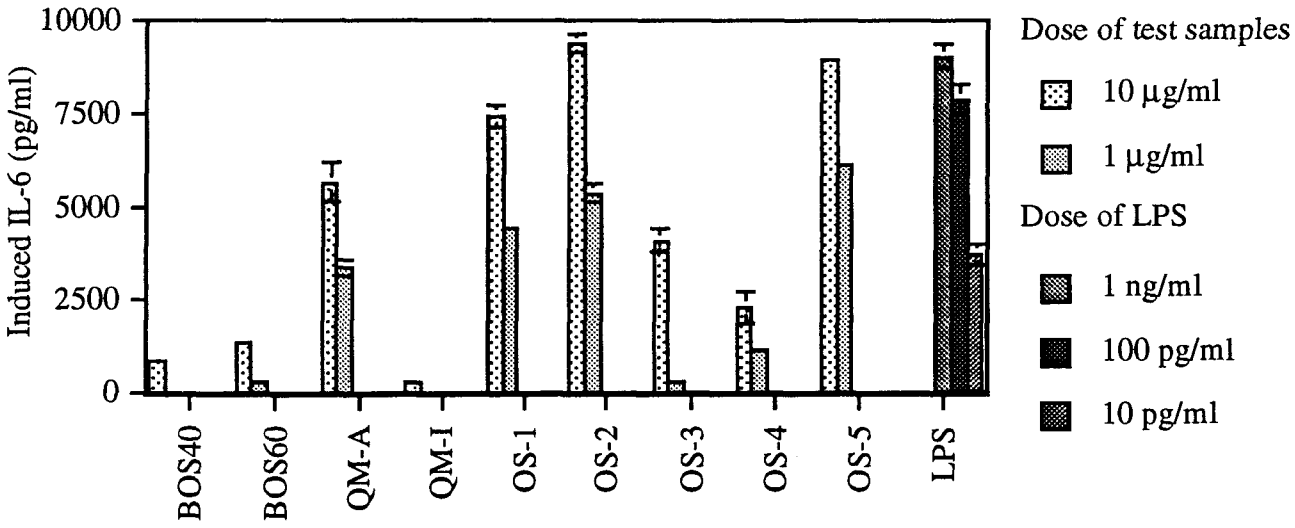

Figure 2-4. IL-6 inducing activity of OS fractions and their parent fractions. Data are means ±SD of two experiments. The blood donor was JY.

propanol. The 1-propanol concentrations selected for elution correspond to those at the peek centers of the two fractions, LTA-1 and LTA-2, in the previous linear gradient elution (*1*). Thus, less hydrophobic fraction (BOS40) and more hydrophobic fraction (BOS60) were obtained from the respective eluates. The yields of BOS15, 40, and 60 were *ca.* 30, 45, and 10%, respectively. The UV spectra of the three fractions proved that only BOS15 contained nucleic acid fragments. As judged from their yield, BOS40 and BOS60 were assumed to correspond to LTA-1 and LTA-2 in the previous work, respectively. IL-6 inducing activity of BOS40 and BOS60 also supported this assumption. Those induced similar amount of IL-6 to those induced by LTA-1 and LTA-2, respectively, as tested with human peripheral whole blood cells (Figure 2-1) in the same manner described previously (*1*).

Further fractionation by ion-exchange membrane chromatography on QMA-Mem Sep 1010 were performed by stepwise elution, because the cytokine-inducing fraction was readily separable in previous work (*1*). The low-anionic cytokine-inducing fraction (QM-A) and the high-anionic fraction (QM-I), which lacks the activity, were obtained from eluates with 0.01 M acetate buffer (pH 4.5) containing 35% 1-propanol and 0.01 M acetate buffer (pH 4.5) containing both 35% 1-propanol and 1 M NaCl, respectively. The average yields of the fractions summarized in Table 2-1 and their IL-6 inducing activity shown in Figure 2-2 are in good agreement to those of the previous study. Since no distinct difference in the IL-6 inducing activity and the chemical composition between QM-A from BOS40 and QM-A from BOS60 was observed, the two fractions were combined for the subsequent study.

The combined QM-A was then subjected to hydrophobic interaction column chromatography on Octyl-Sepharose CL-4B according to the method of Suda *et al.* (*1*) (Figure 2-3 shows the elution profile) to give five fractions, OS-1 to OS-5. The yield of OS-4 was higher than those of other fractions and also higher than that of the corresponding fraction in the previous work (*1*). The IL-6 inducing activity of the fractions were summarized in Figure 2-4. The activity of OS-3 was reduced and especially that of OS-4 were significantly low. As

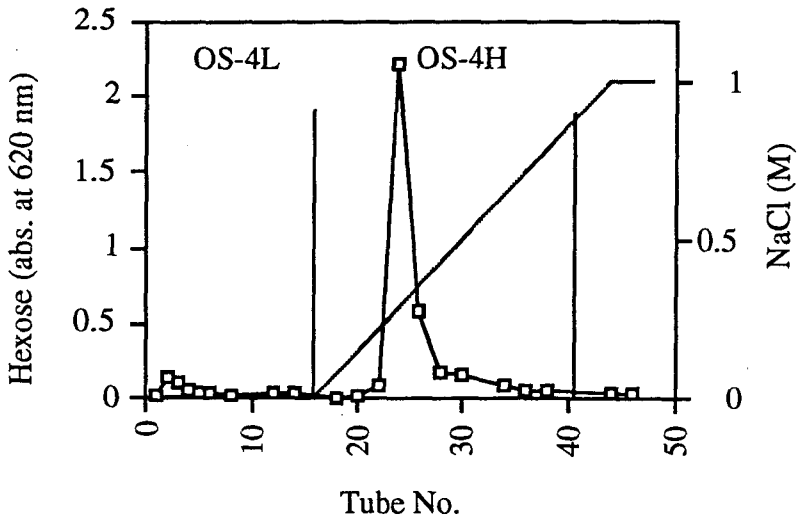

Figure 2-5. The elution profile of OS-4 on QMA-Mem Sep 1010.

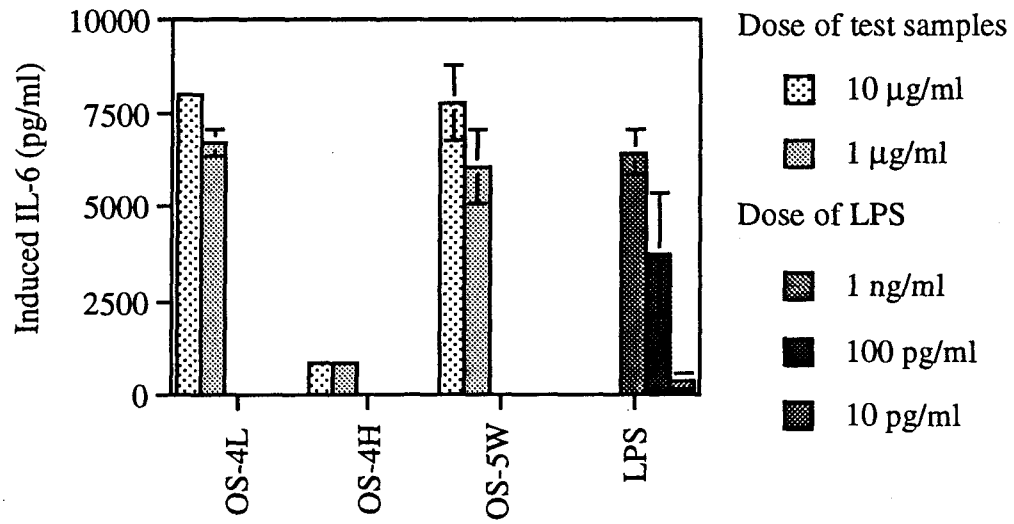

Figure 2-6. IL-6 inducing activity of some purified fractions. Data are means ±SD of two experiments. The blood donor was JY.

Table 2-2. Biological activities of the final fractions.

	QM-A[a)]	QM-I[a)]	OS-1	OS-3	OS-4L	OS-4H	OS-5W
Yield (%)[b)]	-	-	8.8	3.9	5.7	27.3	2.7
IL-6 inducing activity ($\times 10^{-4}$ g/g)[c)]	80	10	160	40	300	10	250
Limulus activity ($\times 10^{-4}$ g/g)[c)]	2.1	2.1	2.9	1.6	1.9	1.9	4.0

a) QM-A is a mixture of QM-A from BOS40 and BOS60. QM-I is from BOS40.
b) The Yield from QM-A.
c) The potency of IL-6 inducing and *Limulus* activity of each specimen is expressed in terms of the corresponding amounts of LPS (from *E. coli* O111:B4, Sigma), as if both IL-6 inducing and *Limulus* activity had been caused by LPS itself.

judged from the fact that QM-I was eluted from Octyl-Sepharose at a similar 1-propanol concentration (40-50%), QM-A might still contain a fraction corresponding to QM-I which lacks a cytokine-inducing activity, if complete separation of QM-A and QM-I on QMA-Mem Sep would have not been accomplished. Thus OS-4 was again subjected to ion-exchange membrane chromatography (Figure 2-5 shows the elution profile) to give a low-anionic fraction (OS-4L) and a high-anionic fraction (OS-4H). The IL-6 inducing activity was found only in the former OS-4L, but not in OS-4H (Figure 2-6), a result showing a contamination of OS-4 with an inactive fraction. OS-4L induced similar extent of IL-6 to that of OS-1. OS-3, which was also anticipated to contain an inactive fraction corresponding to QM-I, was not further purified because of its low quantity. OS-5 was oily and poorly soluble in water, suggesting a contamination of free fatty acids and other lipophilic impurities from Octyl-Sepharose. Thus OS-5 was partitioned with chloroform-methanol-water (2/3/1, v/v/v) to give a water-soluble and IL-6 inducing fraction (OS-5W) from the aqueous phase as white powder and a lipophilic fraction containing fatty acids in the organic phase.

The yields, IL-6 inducing activity and *Limulus* activity of the final fractions are summarized in Table 2-2. In the Table, the potency of IL-6 inducing activity and *Limulus* activity were expressed in terms of the corresponding amounts of LPS as if both activities had been caused by LPS itself. The amounts of LPS calculated on the basis of the *Limulus* activity were at least 50 times smaller than those obtained from IL-6 inducing activity. This fact strongly suggests that the IL-6 inducing activity of the final fractions separated above were inherent in themselves: the presence of contaminating LPS was unequivocally excluded.

In conclusion of this chapter, a rapid and efficient separation method applicable to large scale experiments has been developed using batch-wise and stepwise elution as summarized in Scheme 2-2. The bacterial cells were delipidated and extracted with hot phenol-water, and the crude extract was digested with RNase and DNase to give crude LTA. Separation of the cytokine- fractions was performed by three successive chromatographic separation and

additional processes. A net weight of 46 mg as the cytokine-inducing fractions (OS-1, OS-2, OS-3, OS-4L, and OS-5W) was separated from *ca.* 1 kg of dried bacterial cells.

REFERENCES

1) Suda, Y., Tochio, H., Kawano, K., Takada, H., Yoshida, T., Kotani, S., and Kusumoto, S. (1995) *FEMS Immunol. Med. Microbiol.* **12**, 97-112.

2) Bartlett, G.R. (1959) *J. Biol. Chem.* **234**, 466-468.

3) Ashwell, G. (1957) *Method Enzymol.* **3**, 73-105.

4) Hirano, T., Taga, T., Nakano, N., Yasukawa, K., Kashiwamura, S., Shimizu, K., Nakajima, K., Pyun, K.H., and Kishimoto, T. (1985) *Proc. Natl. Acad. Sci. USA* **82**, 5490-5494.

5) Matsuda, T., Hirano, T., and Kishimoto, T. (1988) *Eur. J. Immunol.* **18**, 951-956.

III. Structural analysis of a major but not cytokine-inducing component

The synthetic LTA analogues (*1*, *2*) which share the fundamental structures proposed for enterococcal and streptococcal LTA (*3*) exhibit neither cytokine-inducing nor antitumor activity (*4*). The structure of the synthetic compounds had several obvious differences from those proposed for natural LTA as described in Chapter I. The lack of the activity in the synthetic compounds might thus be attributed to any of the structural differences. Recent work of Suda *et al.*, however, strongly suggested that not the so-called LTA with the proposed structure but unidentified components are responsible for the cytokine-inducing activity of natural LTA extracted from bacterial cells. They separated the LTA fraction from *E. hirae* ATCC 9790 into cytokine-inducing minor components and an non-inducing major fraction which amounts to over 90 wt% of the original LTA (*5*). This result was confirmed by the present work as described in Chapter II.

In this chapter, the result of the structural study of the inactive major fraction in the LTA fraction is described, which was undertaken to clarify the reason for the negative activity of the synthetic LTA analogues.

MATERIALS AND METHODS

Analytical procedures

1. Phosphorus

Phosphorus contents were determined as the method described in Chapter II.

2. Fatty acids

Fatty acids were analyzed according to the method of Ikemoto *et al.* (*6*). In a test tube, 100 μl of a sample solution (1 mg/ml) and 20 μl of an eicosanoic acid solution (1 mg/ml in methanol) as an internal standard were placed and lyophilized. After addition of methanol containing 5% hydrogen chloride (1 ml; Nakalai Tesque, Inc., Kyoto, Japan), the test tube was sealed under nitrogen atmosphere and heated at 100°C for 2 h. After cooling, the reaction mixture was partitioned with 0.5 ml of water and 1 ml of hexane. The upper hexane phase containing fatty acid methyl esters was separated. The aqueous phase was washed four more times with each 1 ml of hexane. All hexane phases were combined, dried over anhydrous sodium sulfate, and concentrated *in vacuo* to dryness with a rotary evaporator. The residue was dissolved in 100 μl of hexane, and then 2 μl of the solution was analyzed by GC.

The apparatus and the conditions for GC were as follow: apparatus, a GC-14 gas chromatograph (Shimadzu) equipped with a C-R7A Chromatopac (Shimadzu) as an integrator; column, a fused silica capillary column DB-1 (30 m x 0.25 mm ID, J&W Scientific, Folsom, CA, USA); carrier gas, helium at a flow rate of 50 ml/min; injection temperature, 230°C; column temperature, 140-240°C; detection, FID.

3. Carbohydrates

The carbohydrate constituents of the samples were analyzed according to the alditol acetate method (*7*) with a slight modification. A test sample (100 μg) and 100 μl of 1 M hydrochloric acid were heated at 100°C in a sealed tube under nitrogen atmosphere for 3 h. After cooling, 50 μg of xylose was added as an internal standard. Hydrolytically liberated fatty acids in the reaction mixture were extracted three times with each 0.5 ml of hexane. After

addition of two drops of 25% aqueous ammonia solution, the basic products in the aqueous phase were extracted three times with each 0.5 ml of diethyl ether. The aqueous phase was concentrated *in vacuo* to dryness with a rotary evaporator. To the residue, 0.5 ml of aqueous sodium borohydride (2 mg/ml) was added. After 1 h, a few drops of acetic acid were added to quench the reaction. The mixture was concentrated *in vacuo*. The residue was dissolved in 1 ml of methanol and concentrated *in vacuo*. This procedure was repeated total three times to remove the remaining water and boric acid. The residue was dissolved in 0.5 ml of acetic anhydride-pyridine (1/1, v/v), heated at 100°C for 30 min, and concentrated *in vacuo*. The residue was partitioned with 0.5 ml of water and 0.5 ml of chloroform. The lower chloroform phase containing alditol acetate was separated, washed three times with each 0.5 ml of water, and concentrated *in vacuo*. The residue was dissolved in 100 μl of acetone, and then 2 μl of the solution was analyzed by GC or GC-MS.

The conditions for GC were similar to those for the fatty acid analysis. The capillary column (SP-2330, 30 m x 0.25 mm ID, SUPELCO Inc., Bellefonte, PA, USA) was used and the column temperature was 150-240°C. The GC-MS analysis was performed using a Shimadzu QP-5000 with a fused silica capillary column SP-2330 (15 m x 0.25 mm ID).

4. Glycerol

Glycerol was analyzed according to the method of Suda *et al.* (*5*). A mixture of test sample (100 μg) and 500 μl of 2 M hydrochloric acid was heated at 100°C in a sealed tube under nitrogen atmosphere for 2 h. After cooling, 50 μg of xylitol was added as an internal standard. Fatty acids in the reaction mixture were removed by extraction five times with each 0.5 ml of hexane. Then the aqueous phase was concentrated *in vacuo* to dryness with a rotary evaporator. The residue was dissolved in 0.5 ml of an alkaline phosphatase solution (2 unit/ml in 0.04 M ammonium carbonate; EC 3.1.3.1, from *E. coli*, Wako Pure Chemical Co. Ltd., Osaka, Japan) and allowed to stand at 37°C for 24 h. The reaction mixture was concentrated *in*

vacuo. The residue was dissolved in 0.3 ml of methanol and concentrated *in vacuo*. This procedure was repeated total five times to remove the remaining water. To the residue, 0.2 ml of pyridine, 40 μl of hexamethyldisilazane, and 20 μl of trimethylchlorosilane were added successively. After 30 min, a part of the solution (2 μl) was analyzed by GC.

The conditions for GC were similar to those used for the fatty acid analysis. The column temperature was 100-240°C. The content in each sample was calculated from the calibration curve obtained with standard glycerol by GC.

5. Amino acids

A test sample (50 μg) and 100 μl of 6 M hydrochloric acid in a test tube were deaerated by freeze-and-thaw cycles. The test tube was sealed under reduced pressure and heated at 110°C for 22 h. After cooling, the reaction mixture was concentrated *in vacuo* to dryness with a rotary evaporator. The amino acids were analyzed by the ninhydrin method using a 655A-12 HPLC (Hitachi Ltd., Tokyo, Japan) equipped with a #2619F column (150 mm x 4 mm ID, Hitachi).

6. Sodium

Sodium content was determined using an Optima 300-XL ICP emission spectrometry (Perkin-Elmer, Norwalk, CT, USA).

7. SDS-PAGE

SDS-PAGE was performed using an AE-6330 apparatus (ATTO, Tokyo, Japan) and a 15% polyacrylamide gel (PAGEL SPU-15S, ATTO) according to the method of Schagger and Jagow (*8*). Samples (6 μg) were dissolved in 20 μl of the sample preparation buffer (described below). After heating at 100°C for 5 min, the sample solutions were applied to wells on the gel. Molecular weight markers (#80-1129-83, Pharmacia) were also applied to a well. The

electrophoresis was run at a constant current (20 mA) for 2 h.

The Alcian blue staining was performed according to the method of Rice (*9*) with a slight modification. The gel was soaked in 100 ml of 0.2% aqueous Alcian blue 8GX (Sigma) containing 1.0 g of $MgCl_2 \cdot 6H_2O$ and 3.0 ml of acetic acid for 5 h and then in 3% acetic acid containing 0.05 M $MgCl_2$ for 5 h and dried *in vacuo*.

The silver staining was performed according to the method of Tsai (*10*) with a slight modification. The gel was soaked in 200 ml of 5% acetic acid containing 40% ethanol for 10 min and then in 200 ml of 5% acetic acid containing both 40% ethanol and 0.7% of periodic acid for 60 min. After washing with water three times, the gel was soaked in the silver nitrate solution (described below) for 10 min. After washing with water three times, the gel was soaked in 0.05% aqueous formaldehyde containing 0.01 g of citric acid until the bands were visualized. The gel was soaked in 200 ml of 10% acetic acid, washed with water twice, and dried *in vacuo*.

The sample preparation buffer was prepared as follows. Sodium dodecyl sulfate (2 g), 2 g of tris(hydroxymethyl)aminomethane, 40 g of glycerol, and 0.02 g of Coomassie brilliant blue were dissolved in 100 ml of water. The solution was stored at 4°C until use.

The silver nitrate solution was prepared as follows. An aqueous ammonia solution (28%, 2 ml) was added to 28 ml of 0.1 M sodium hydroxide. After addition of aqueous silver nitrate (20%, 5 ml), the solution was dilued with 115 ml of water.

Image scanning of the stained gels and data processing were performed by a Power Macintosh 8100/100 (Apple Japan, Inc., Tokyo, Japan) equipped with an image scanner ScanJet IIcx (Hewlett Packard, San Diego, CA, USA) using a PhotoShop 2.5J software (Adobe System Japan, Tokyo, Japan).

8. TLC

TLC was performed on silica-gel plates (Merck Keiselgel 60 F_{254} Art. 5715). The

following solvent systems were used: A, chloroform-methanol-water (65/25/4, v/v/v); B, chloroform-methanol-ethyl acetate (100/4/6, v/v/v). Spots on the plate were visualized by the use of iodine vapor, water spray, or an anisaldehyde-sulfuric acid reagent. The TLC plates were scanned and the image data were processed as described for the SDS-PAGE.

9. HPLC

HPLC was carried out on an LC-6AC liquid chromatograph (Shimadzu) equipped with an RID-6A refractive index detector (Shimadzu) and a C-R7A Chromatopac (Shimadzu) as an integrator. The gel permeation chromatography was performed on an Asahipak GFA-30 column (500 mm x 7.5 mm ID; Asahi Kasei, Kanagawa, Japan) using 0.01 M phosphate buffer (pH 7.0) containing 0.5 M NaCl as an eluent at a flow rate of 0.8 ml/min. Several heparin standards (molecular weights: 1.8×10^4, 9.8×10^3, 4.4×10^3, 2.4×10^3, and 1.2×10^3) and dextran standards (1.7×10^4, 1.15×10^4, and 9.4×10^3) were used to make calibration curves for the estimation of the molecular weight.

NMR spectroscopy

Proton, ^{13}C, and ^{31}P NMR spectra were measured on a JMN-LA500 spectrometer (JEOL, Tokyo, Japan) at 500, 126, and 202 MHz, respectively. The chemical shifts are expressed in δ values by using tetramethylsilane (δ 0) or water (δ 4.65) as an internal standard for ^1H spectra, and tetramethylsilane (δ 0) as an internal or benzene (δ 128) as an external standard for ^{13}C spectra, and 85% phosphoric acid (δ 0) as an external standard for ^{31}P spectra. Unless otherwise noted, two dimensional heteronuclear experiments were performed between ^1H and ^{13}C.

Mass spectrometry

FAB-MS spectra were obtained with an SX-102 mass spectrometer (JEOL). Glycerol

or *m*-nitrobenzyl alcohol was used as a matrix. ESI-MS spectra were obtained with an API III plus mass spectrometer (PE SCIEX, Thornhill, Ontario, Canada). MALDI-TOF-MS spectra were obtained with a Kratos Kompact MALDI IV (Shimadzu) mass spectrometer. 2,5-Dihydroxybenzoic acid or a mixture of 2,5-dihydroxybenzoic acid and 5-methoxysalicylic acid (10/1, w/w) was used as a matrix.

Deacylation of the inactive major fraction (QM-I)

Deacylation of QM-I was performed according to the procedure of Kochanowski *et al.* (*11*). QM-I (10 mg) was hydrolyzed with 1 ml of 0.2 M aqueous sodium hydroxide at 37°C for 2 h. Liberated fatty acids in the reaction mixture were extracted four times with each 1 ml of a mixture of hexane-chloroform (5/1, v/v). The aqueous phase was dialyzed and lyophilized to give deacylated product.

Determination of phosphomonoester in the inactive major fraction (QM-I)

QM-I (1.5 mg) was dissolved in 1.5 ml of an alkaline phosphatase solution (5 unit/ml in 0.04 M ammonium carbonate; Wako). The mixture was incubated at 37°C for 24 h. Liberated phosphate in the reaction mixture was determined by the method described above.

Hydrolysis of the inactive major fraction (QM-I)

Hydrolysis of QM-I with 47% hydrofluoric acid and phase partition of the reaction products were performed according to the procedure of Fischer (*4*). QM-I (10 mg) was hydrolyzed with 50 µl of 47% hydrofluoric acid at 4°C for 24 h. The reaction mixture was dried *in vacuo* over sodium hydroxide. The residue was partitioned with 1 ml of a two-phase solvent system composed of chloroform, methanol, and water (2/1/3, v/v/v). Both the aqueous and the organic phase were concentrated separately *in vacuo* to dryness with a rotary evaporator. The products in the organic phase was separated by TLC using solvent system A.

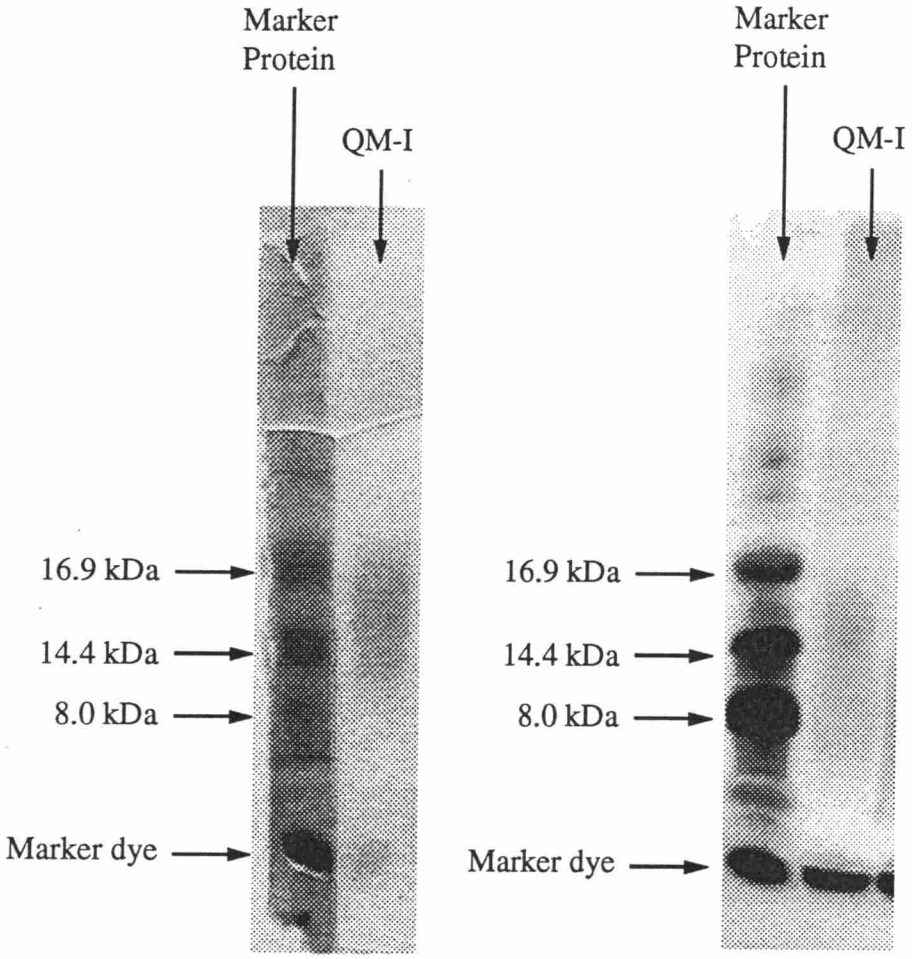

Figure 3-1. The SDS-PAGE Profiles of the compound in QM-I from BOS40. The left gel was visualized by Alcian blue staining and the right one was by silver staining. The stained patterns were scanned by an image scanner.

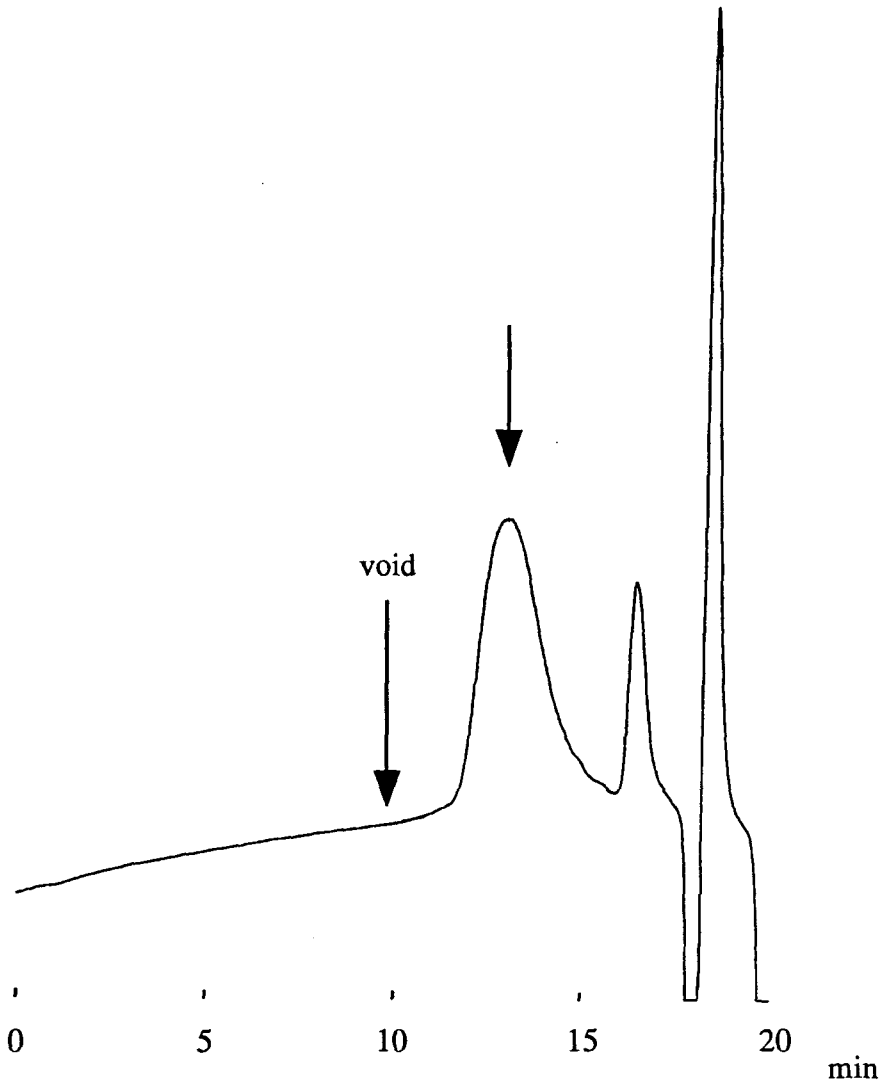

Figure 3-2. The elution profile of the deacylated product of QM-I from BOS40 on gel permeation HPLC. The peaks and troughs after 16 min are due to turbulence by the solvent system.

The products in the aqueous phase were treated with 0.5 ml of an alkaline phosphatase solution (2 unit/ml in 0.04 M ammonium carbonate) at 37°C for 24 h. After lyophilization, the residue was peracetylated with 0.5 ml of a mixture of acetic anhydride-pyridine (1/1, v/v) at room temperature for 24 h. After evaporation *in vacuo*, the peracetylated products were partitioned with 1 ml of chloroform and 1 ml of water. The organic phase was washed three times with each 1 ml of water and concentrated *in vacuo*. The residue was separated by TLC using solvent system B.

RESULTS AND DISCUSSION

Chemical structure of the compound in the major but not cytokine-inducing fraction QM-I from the BOS40 fraction of LTA (Scheme 2-2, p. 15) was studied.

The SDS-PAGE profile of the compound in QM-I is shown in Figure 3-1. In both silver and Alcian blue stainings one broad band was visualized in the molecular weight range of 1.2-1.6 x 10^4. HPLC analysis of the compound in QM-I itself was not successful probably because of its micellar aggregation. Deacylated product was eluted as a broad but single peak in gel permeation HPLC (Figure 3-2). Its molecular weight was estimated to be in the range of 2-8 x 10^3 (calculated from heparin standards) or 7-14 x 10^3 (calculated from dextran standards). Attempts to determine the molecular weight of both native compound and deacylated product of QM-I by ESI-MS or MALDI-TOF-MS was not successful. Although the exact value was not determined, the molecular weight was roughly estimated to be around 1 x 10^4. QM-I is also hydrophobically and anionically homogeneous as judged from their elution profiles in the corresponding chromatographies. QM-I therefore is thought to contain a single kind of macromolecular glycoconjugate with the above-mentioned molecular weight range due to the presence of homologues. The chemical composition of the glycoconjugate is

Table 3-1. Chemical composition of the glycoconjugate in QM-I. Molar ratios were calculated by assuming the presence of two moles of fatty acids.

	Wt%	(Molar ratio)
Phosphate	11.5	(12.0)
Glycerol	18.7	(14.0)
Glucose	42.4	(17.3)
Fatty Acid	7.6	(2.0)
C16:0		(0.7)
C16:1		(0.1)
C18:0		(0.2)
C18:1		(0.9)
Alanine	2.3	(2.0)

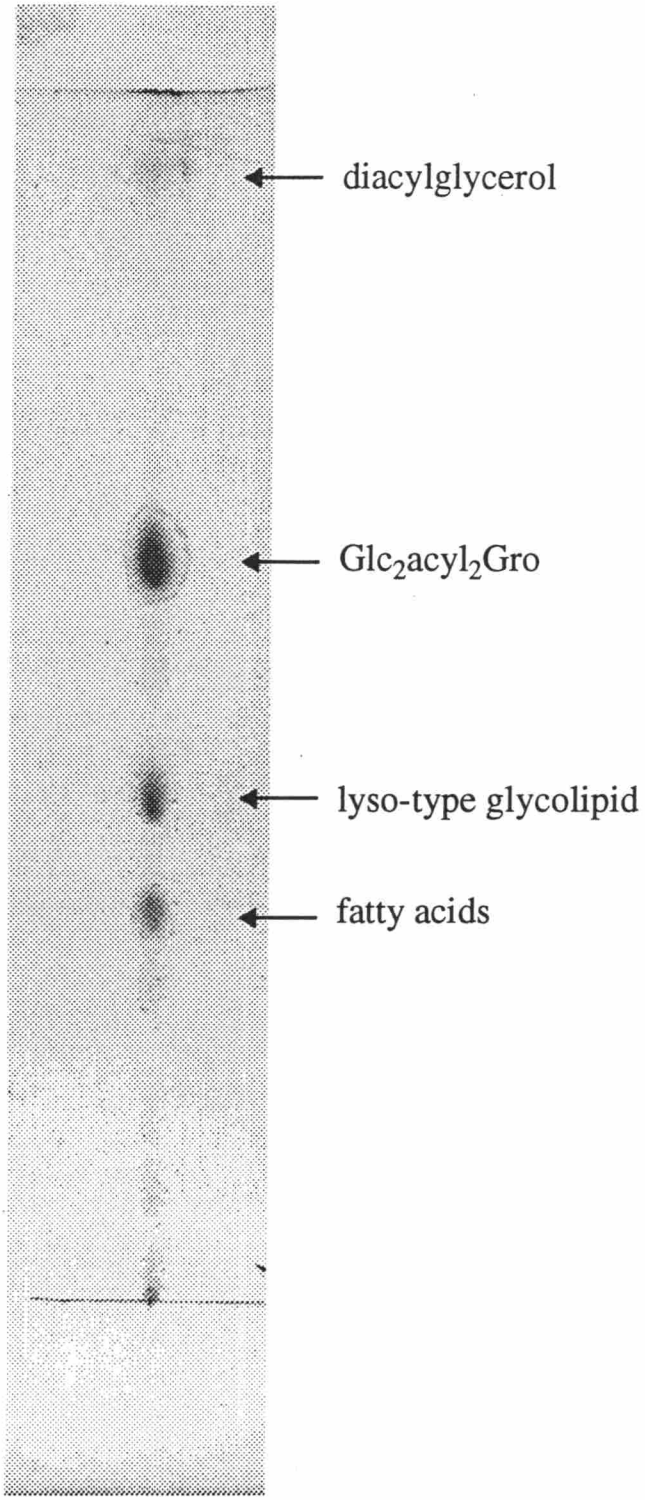

Figure 3-3. A TLC profile of the products extracted in the organic phase from the HF-hydrolysate of the glycoconjugate in QM-I. TLC was done on a silica gel plate (Merck Keiselgel 60 F_{254} Art. 5715) using solvent system A: chloroform-methanol-water (65/25/4, v/v/v). The spots were visualized with an anisaldehyde-sulfuric acid reagent.

Table 3-2. ^1H NMR data for the glycolipid Glc_2acyl_2Gro obtained by HF-hydrolysis of the glycoconjugate in QM-I and a synthetic counterpart of the former. The spectra were measured in $CDCl_3$-CD_3OD (3/1) at 303K. The assignments were established by ^1H and ^{13}C one-dimensional spectroscopy, one-dimensional ^1H NOE, and the following two-dimensional methods: DQF-COSY, NOESY, TOCSY, and HMQC. Glc^r and Glc^{nr} stand for the reducing and non-reducing side glucose residues, respectively. The data for synthetic glycolipid were taken from reference (*1*).

Proton	Glc_2acyl_2Gro		Synthetic glycolipid	
	Chemical shift ($^3J_{H,H}$)		Chemical shift ($^3J_{H,H}$)	
	δ	(Hz)	δ	(Hz)
Glycerol				
Gro H-1	4.20	(6.6, 12.2)	4.20	(6.4, 12.1)
	4.43	(3.4, 12.2)	4.43	(3.0, 12.1)
Gro H-2	5.23		5.23	
Gro H-3	3.64	(5.1, 10.8)	3.64	(5.3, 10.6)
	3.83	(5.3, 10.9)	3.83	(5.8, 10.6)
Glucose				
Glc^r H-1	4.98	(3.5)	4.98	(3.6)
Glc^r H-2	3.59	(3.5, 9.8)	3.58	(3.6, 9.6)
Glc^r H-3	3.78	(8.9, 9.8)	3.78	
Glc^r H-4	3.45	(8.9, 9.7)	3.44	(9.2, 9.9)
Glc^r H-5	3.57		3.57	
Glc^r H-6	3.78		3.7-3.8	
Glc^{nr} H-1	4.95	(3.8)	4.95	(3.8)
Glc^{nr} H-2	3.45	(3.9, 9.6)	3.44	(3.8, 9.5)
Glc^{nr} H-3	3.70	(9.0, 9.6)	3.69	(9.2, 9.5)
Glc^{nr} H-4	3.33	(9.1, 9.8)	3.34	(9.2, 9.5)
Glc^{nr} H-5	3.88		3.88	
Glc^{nr} H-6	3.69	(6.1, 12.2)	3.70	(6.2, 12.4)
	3.86		3.86	

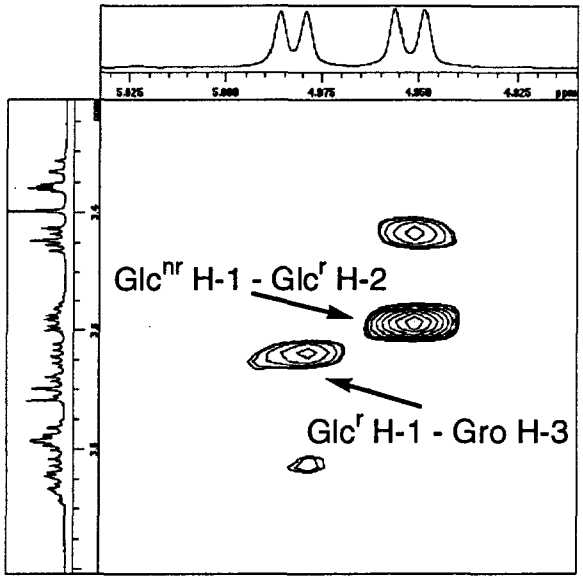

Figure 3-4. A part of the NOESY spectrum of Glc_2acyl_2Gro. The spectrum was measured in $CDCl_3$-CD_3OD (3/1, v/v) at 303K. The mixing time was 650 ms.

summarized in Table 3-1. Since no liberated free phosphate was detected by the direct alkaline phosphatase digestion of the glycoconjugate, the presence of phosphomonoester was excluded. The phosphorus in the molecule was thus concluded to exist in the phosphodiester form. The molar ratio of phosphorus to glycerol was approximately 1, suggesting the existence of the poly(glycerophosphate) structure.

To cleave phosphodiester linkages expected to be abundantly present in the molecule, the glycoconjugate in QM-I was subjected to hydrofluoric acid (HF) hydrolysis and the products were partitioned with a mixture of chloroform-methanol-water (2/1/3, v/v/v). On TLC analysis using solvent system A, one major and several minor products were detected in the organic phase of the HF-hydrolysate (Figure 3-3). They were isolated by TLC. Their positive mode FAB-MS and ^{1}H NMR spectra revealed that the major product has a Glc_2acyl_2Gro structure, and the minor ones are the corresponding lyso derivative, diacylglycerol, and fatty acids.

One-dimensional ^{1}H NMR data for the glycerol and glucose residues in Glc_2acyl_2Gro is summarized in Table 3-2. The coupling constants of the protons at the 1 to 4-positions of both glucose residues indicated their pyranosyl structures (*12*). The chemical shifts (δ 4.98 and 4.95) and the coupling constants (3.5 and 3.8 Hz as $^3J_{1,2}$) of the anomeric protons confirmed the α-configurations (*13*). With regard to the glycerol residue, the downfield shifts of the H-1 and H-2 in comparison with the H-3 indicated that the fatty acids are located at the 1- and 2-positions. In the NOESY spectrum of QM-I shown in Figure 3-4, interresidual NOEs between Glc^{nr} H-1 and Glc^r H-2, and Glc^r H-1 and Gro H-3 were observed (Glc^{nr} stands for the non-reducing side glucose and Glc^r for the reducing side glucose). On peracetylation, no downfield shift of Glc^r H-2 was observed in the ^{1}H NMR spectrum (data not shown). From these results, the glycolipid structure was determined as $Glc^{nr}(\alpha 1\text{-}2)Glc^r(\alpha 1\text{-}3)acyl_2Gro$. These NMR data were in good agreement with those of the corresponding synthetic counterpart (*1*) cited in Table 3-2. This NMR spectroscopic identification also proves the stereochemistry of

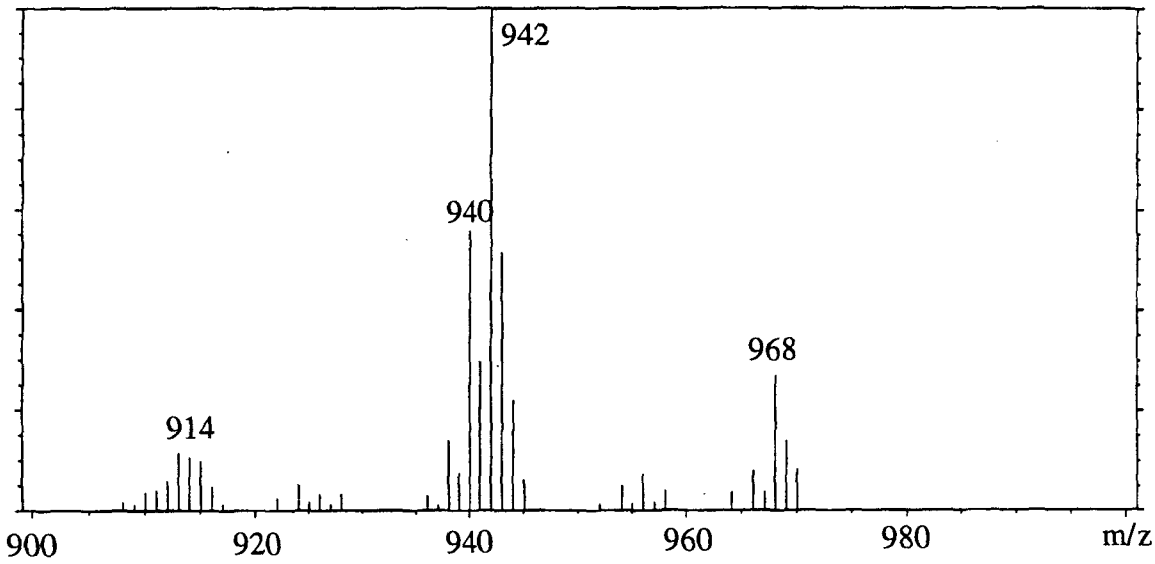

Figure 3-5. FAB-MS analysis of Glc_2acly_2Gro. m-Nitrobenzyl alcohol was used as a matrix. For example, the ion peaks at m/z 914, 940, 942, and 968 correspond to a glycolipid with a hexadecanoic and a hexadecenoic, a hexadecenoic and a octadecanoic, a hexadecanoic and a octadecenoic, and two octadecenoic acids, respectively.

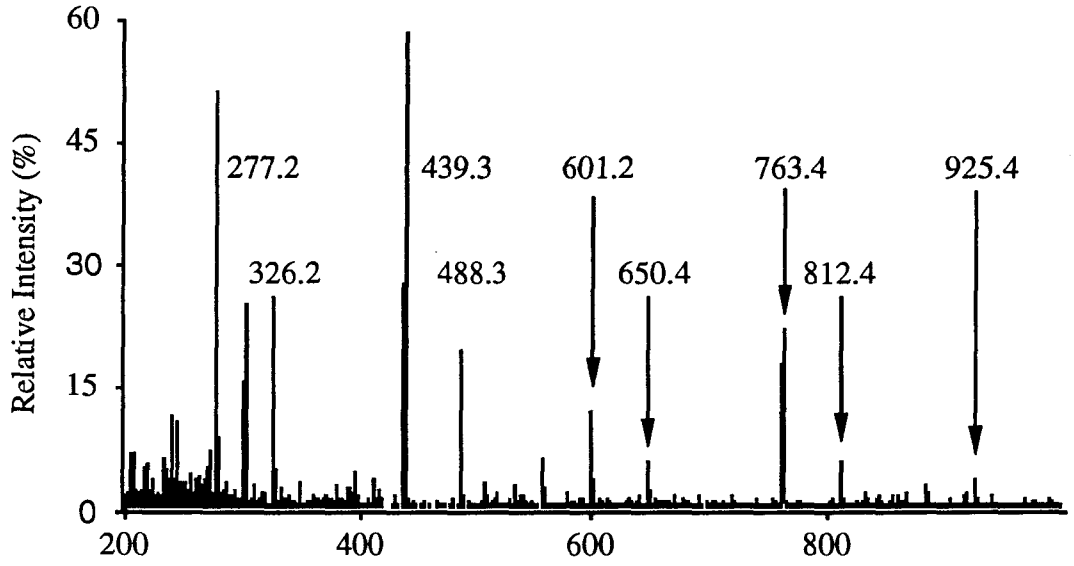

Figure 3-6. Positive mode ESI-MS analysis of the products extracted in the aqueous phase from the HF-hydrolysate of the glycoconjugate in QM-I. A 0.1 mg/ml solution (in 20% aqueous 2-propanol) was continuously infused at 0.3 ml/h.

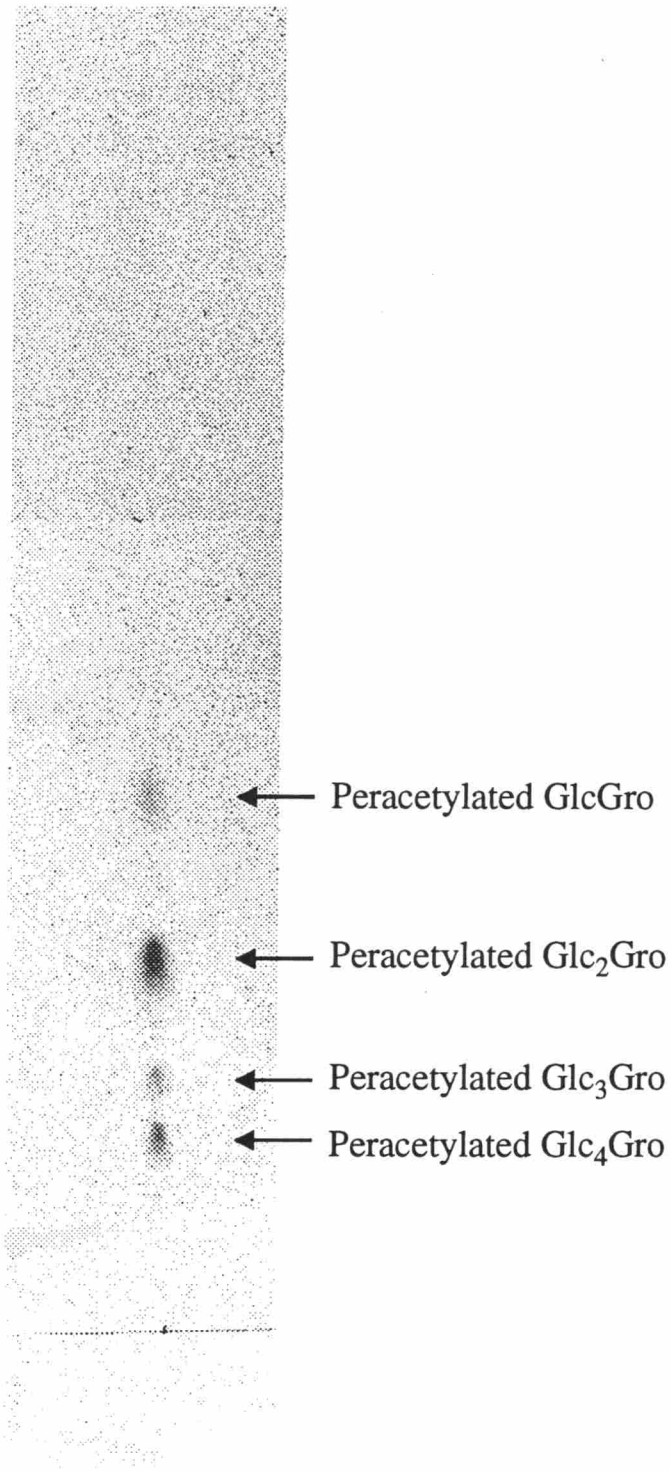

Figure 3-7. TLC analysis after peracetylation of the products extracted in the aqueous phase from the HF-hydrolysate of the glycoconjugate in QM-I. TLC was done on a silica gel plate (Merck Keiselgel 60 F_{254} Art. 5715) using solvent system B: chloroform-methanol-ethyl acetate (100/4/6, v/v/v). The spots were visualized with an anisaldehyde-sulfuric acid reagent. Peracetylated Gro, not visualized by this method, was detected with iodine vapor (data not shown).

the glycerol residue in the glycoconjugate in QM-I to be the same as present in the common glycoglycerolipids (*3*).

The fatty acid esters in the glycolipid, Glc_2acyl_2Gro, were mainly composed of hexadecanoate, hexadecenoate, octadecanoate, and octadecenoate in the molar ratio of 0.63/0.23/0.10/1.00. Positive ion mode FAB-MS analysis of the glycolipid showed the molecular ion peaks depicted in Figure 3-5. The heterogeneity of the molecular weight is explained by the substitution with different combinations of fatty acids at the 1- and 2-positions of the glycerol: *e.g.*, the peak at m/z 942 corresponds to a glycolipid with one hexadecanoic and one octadecenoic acid, whereas the peak at m/z 968 contains two octadecenoic acids.

The products extracted in the aqueous phase from the HF-hydrolysate were analyzed by ESI-MS. In the positive ion mode, two series of ion peaks at m/z 277.2, 439.3, 601.2, 763.4, 925.4 and m/z 326.2, 488.3, 650.4, 812.4 were observed (Figure 3-6). The former series was assigned to sodium adducts of Glc_nGro (n=1-5) and the latter to $AlaGlc_nGro$ (n=1-4) in its protonated form. Since the negative ion mode ESI-MS indicated the presence of compounds which still retained phosphate groups, the mixture was further treated with an alkaline phosphatase to remove the remaining phosphates. In the ESI-MS analysis (positive ion mode) of the resulting dephosphorylated products, only the molecular ion peaks of the sodium adducts of Glc_nGro (n=1-5) were observed and the alanine substituents were no longer detected. Since the phosphatase treatment was undertaken under weakly alkaline conditions, the disappearance of the alanine residues suggests that they were linked to Glc_nGro through ester linkages. The dephosphorylated products were peracetylated and five compounds were isolated by TLC using solvent system B (the pattern of analytical TLC is shown in Figure 3-7). The isolated compounds were characterized on the basis of ^{1}H-NMR spectra as peracetylated Gro, $Glc^{I}(\alpha 1\text{-}2)Gro$, $Glc^{II}(\alpha 1\text{-}2)Glc^{I}(\alpha 1\text{-}2)Gro$, $Glc^{III}(\alpha 1\text{-}2)Glc^{II}(\alpha 1\text{-}2)Glc^{I}(\alpha 1\text{-}2)Gro$, and $Glc^{IV}(\alpha 1\text{-}2)Glc^{III}(\alpha 1\text{-}2)Glc^{II}(\alpha 1\text{-}2)Glc^{I}(\alpha 1\text{-}2)Gro$. (Glucosyl residues are numbered from the one linked to the glycerol to the non-reducing terminus.) In spite of its detection in ESI-MS

Table 3-3. ^1H NMR data for peracetylated Gro, GlcGro, Glc_2Gro, Glc_3Gro, Glc_4Gro. The spectra were measured in $CDCl_3$ at 303K. The assignments were established by ^1H and ^{13}C one-dimensional spectroscopy, DQF-COSY, and HMQC. Glucosyl residues are numbered from that linked to the glycerol and to the non-reducing terminus.

Proton	Chemical shifts δ (Coupling constants) (Hz)				
	Gro	GlcGro	Glc_2Gro	Glc_3Gro	Glc_4Gro
Gro H-1	4.16 (5.7, 11.9)	4.09	4.18	4.18	4.09
	4.29 (4.1, 11.9)	4.27	4.28	4.38	4.43
Gro H-2	5.24	4.06	4.09	4.26	4.18
Gro H-3	4.16 (5.7, 11 9)	4.09	4.21	4.17	4.24
	4.29 (4.1, 11 9)	4.27	4.27	4.33	4.30
Glc^I H-1		5.31 (3.9)	5.21 (3.7)	5.33 (3.9)	5.34 (3.9)
Glc^I H-2		4.84 (3.8, 10.3)	3.75 (3.6, 9.9)	3.73 (3.9, 10.1)	3.93 (3.7,9.9)
Glc^I H-3		5.47 (9.6, 10.1)	5.45 (9.4, 9.8)	5.45 (9.6, 9.6)	5.49 (9.4,9.6)
Glc^I H-4		5.06 (9.8, 9.9)	4.98 (9.2, 10.3)	5.00 (9.6, 9.9)	5.04 (9.1, 9.4)
Glc^I H-5		4.20	4.21	4.26	4.27
Glc^I H-6		4.17	4.05	4.06	4.11
		4.23 (4.6, 12.4)	4.29	nd	nd
Glc^{II} H-1			5.16 (3.5)	5.04 (3.2)	5.05 (3.0)
Glc^{II} H-2			4.87 (3.5,10.4)	3.76 (3.2, 10.3)	3.70 (3.2, 10.3)
Glc^{II} H-3			5.37 (9.5, 10.2)	5.40 (9.6, 9.9)	5.33
Glc^{II} H-4			5.07 (9.5, 10.2)	4.99 (9.6, 10.1)	5.00 (9.6, 9.9)
Glc^{II} H-5			4.07	4.16	4.04
Glc^{II} H-6			4.16	4.07	nd
			nd	4.18	nd
Glc^{III} H-1				5.10 (3.7)	5.20 (3.4)
Glc^{III} H-2				4.94 (3.7, 10.3)	3.76 (3.4, 9.9)
Glc^{III} H-3				5.32 (9.4, 10.3)	5.35
Glc^{III} H-4				5.08 (9.4, 10.1)	5.01 (9.6, 10.0)
Glc^{III} H-5				4.11	4.08
Glc^{III} H-6				4.18	4.17
				nd	nd
Glc^{IV} H-1					5.12 (3.9)
Glc^{IV} H-2					4.92 (3.6, 10.2)
Glc^{IV} H-3					5.31
Glc^{IV} H-4					5.10 (9.6, 10.1)
Glc^{IV} H-5					4.00
Glc^{IV} H-6					4.19

nd: not determined because of signal overlapping.

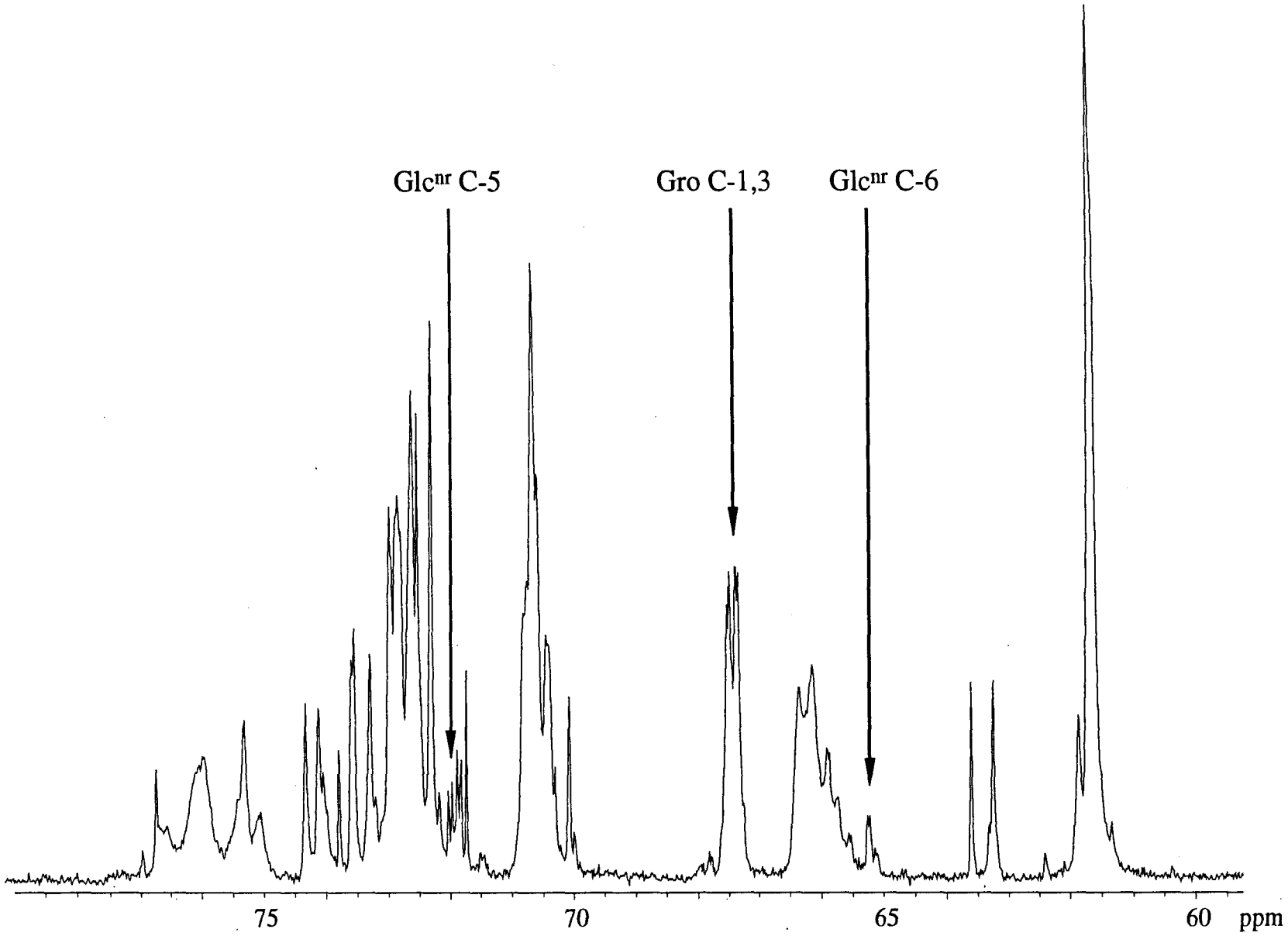

Fig. 3-8. ^{13}C NMR spectrum of deacylated product of the glycoconjugate in QM-I. The spectrum was measured in D_2O at 303K. The assignments were established by DEPT (135°), HMQC, HMBC, DQF COSY, TOCSY, and NOESY. Glc^{nr} means the non-reducing side glucose of the glycolipid region.

Table 3-4. ^{1}H and ^{13}C NMR data for the glycerol and glucose residues of the glycolipid region in the deacylated product of QM-I. The spectra were measured in D_2O at 303K. The assignments were established by ^{1}H and ^{13}C one-dimensional spectroscopy, one-dimensional TOCSY, and the following two-dimensional methods: DQF-COSY, TOCSY, HMQC, and HMBC as well as by reference to the data (*12*). Glc^{r} stands for the glucose residue of the reducing side, Glc^{nr} for that of the non-reducing side.

Position	Chemical shifts (δ)	
	^{1}H	^{13}C
Gro 1	3.65	64.62
Gro 2	nd	71.52
Gro 3	3.81	70.00
Glc^{r} 1	5.11	97.15
Glc^{r} 2	3.63	76.74
Glc^{r} 3	3.76	72.55
Glc^{r} 4	3.42	70.69
Glc^{r} 5	3.54	72.55
Glc^{r} 6	3.67	61.88
	3.76	
Glc^{nr} 1	5.04	97.40
Glc^{nr} 2	3.56	72.33
Glc^{nr} 3	3.73	73.80
Glc^{nr} 4	3.50	70.69
Glc^{nr} 5	3.97	72.01
Glc^{nr} 6	4.06	65.25

nd: not determined because of signal overlapping.

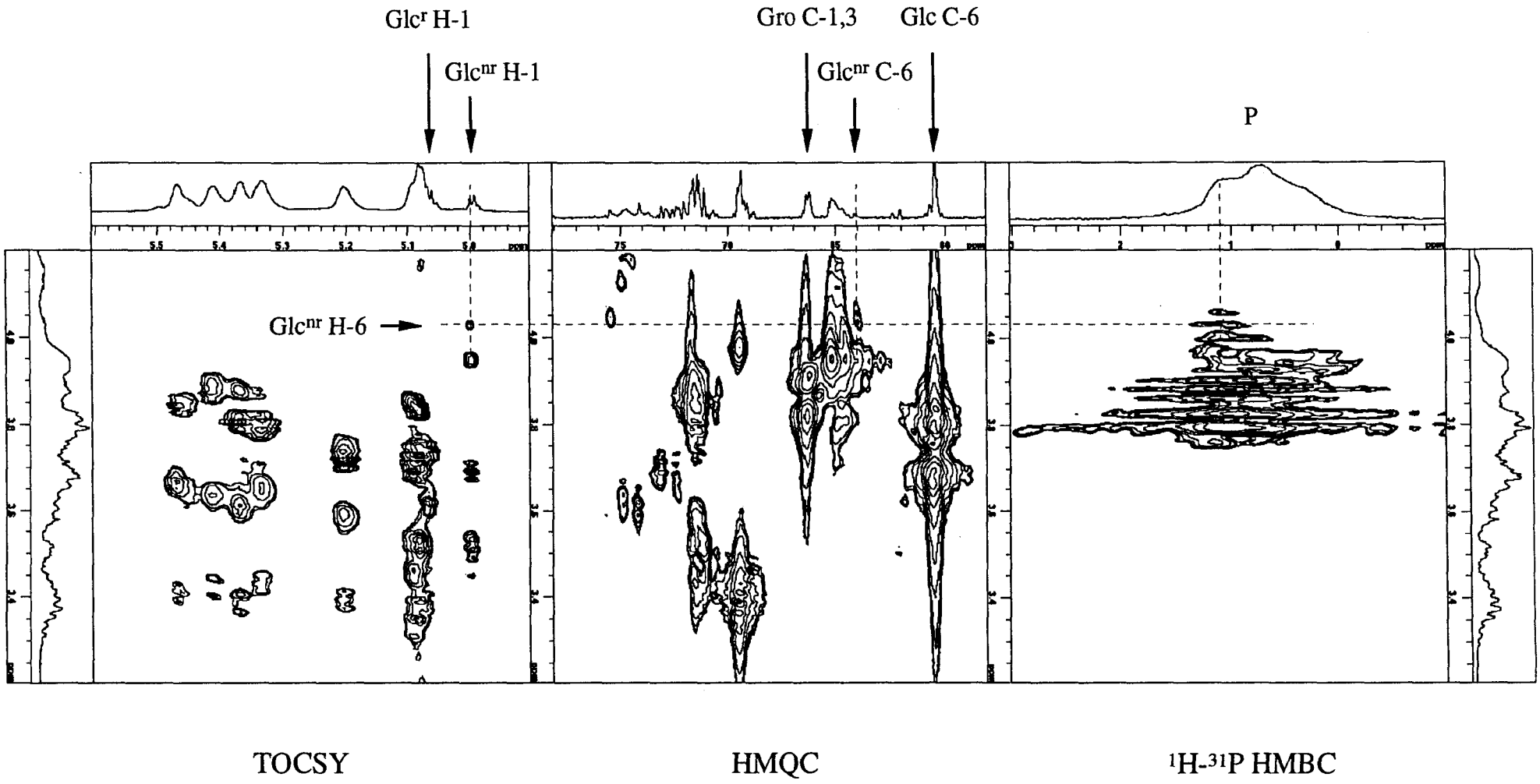

Figure 3-9. A part of TOCSY, HMQC, and ^{1}H-^{31}P HMBC spectra of deacylated product of the glycoconjugate in QM-I. The spectra were measured in D_2O at 303K.

mentioned above, the presence of Glc_5Gro was not observed on TLC because of its low content. Proton NMR data of these components are summarized in Table 3-3. The coupling constants of the anomeric and other ring protons indicated α-glucopyranosyl configurations for all glucose residues. No downfield shifts of Gro H-2 were observed on peracetylation of Glc_nGro, indicating the Glc(α1-2)Gro linkages. No downfield shifts were observed for Glc^{I} H-2 and Glc^{II} H-2 of peracetylated Glc_3Gro either. This proves the Glc(α1-2)Glc linkages in Glc_nGro. The positions of interresidual linkages were further confirmed by HMBC. Thus, the expected interresidual correlations in peracetylated Glc_2Gro were observed between Glc^{II} C-1 and Glc^{I} H-2, Glc^{II} H-1 and Glc^{I} C-2, Glc^{I} C-1 and Gro H-2, and Glc^{I} H-1 and Gro C-2.

To elucidate the mode of connection between the glycolipid and the Glc_nGro moiety in QM-I, the NMR spectra of the deacylated product of QM-I were examined. The ^{13}C NMR spectrum is shown in Figure 3-8. The signals at δ 67.38 and 67.52 with coupling constants of *ca.* 5 Hz are assigned to Gro C-1 and -3. The downfield shifts and the coupling constants corresponding to a value expected for $^{2}J_{c,p}$ indicate phosphodiester linkages at the 1 and 3-positions of glycerol and, therefore, prove the presence of a 1,3-phosphodiester-linked poly(glycerophosphate) chain. The ^{1}H and ^{13}C NMR for the glycolipid region are summarized in Table 3-4. The assignments were established by DEPT (135°), TOCSY, NOESY, HMQC, and HMBC spectra and by referring the reported data (*11*). The observed coupling constants of Glc^{nr} C-6 (*ca.* 5 Hz) and Glc^{nr} C-5 (*ca.* 7 Hz) coincide with the values expected for $^{2}J_{c,p}$ and $^{3}J_{c,p}$, respectively. This unequivocally proves the phosphodiester linkage at the 6-position of the non-reducing side glucose. Furthermore, the cross-peak between Glc^{nr} H-6 and a ^{31}P signal detected by ^{1}H-^{31}P HMBC spectrum (Figure 3-9) also supports this conclusion. From these results, it became evident that the poly(glycerophosphate) chain is linked to the 6-position of the non-reducing side glucose in the glycolipid moiety.

Taking all the data into account, the chemical structure of the glycoconjugate in QM-I, the major but not cytokine-inducing component in BOS40 from *E. hirae* ATCC 9790, was

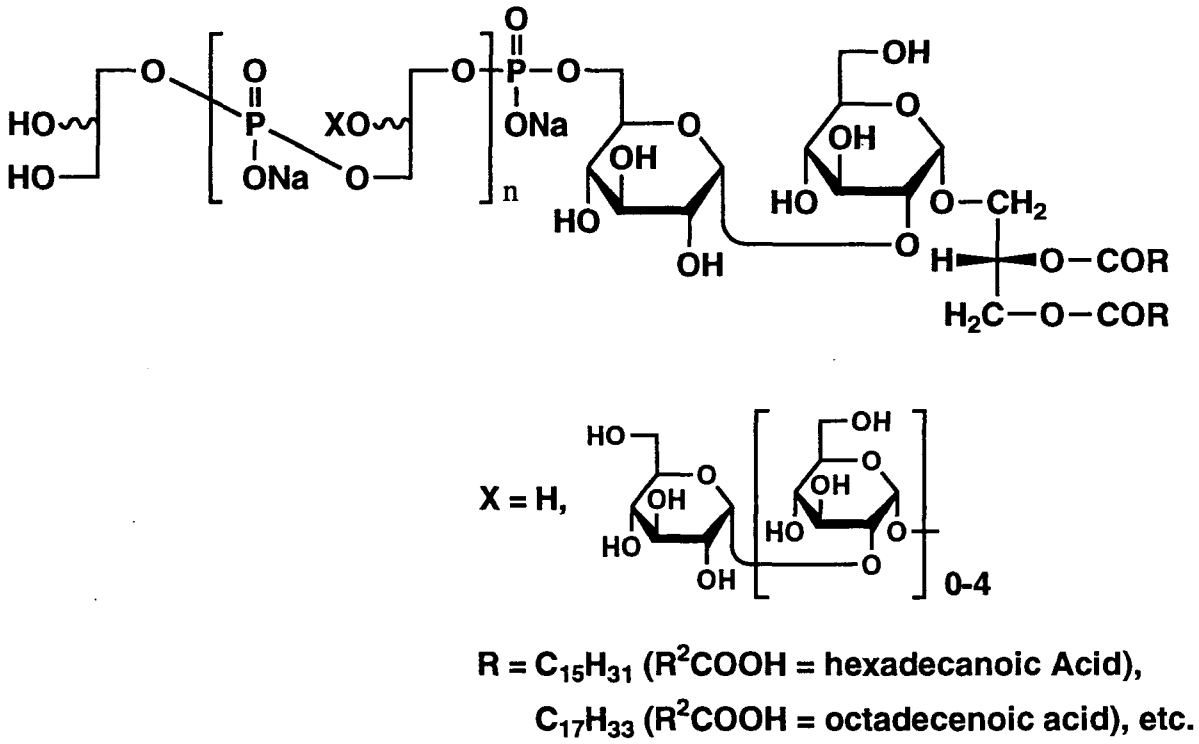

Figure 3-10. The structure of the glycoconjugate in QM-I from BOS40. A part of the oligoglucosyl substituents on glycerols may be further substituted with alanine.

deduced to be as shown in Figure 3-10, except for the location of the alanyl substitution and the stereochemistry of the glycerols in poly(glycerophosphate) moiety. The structure coincides with the one proposed by Fischer's group for LTA-1 isolated from the same bacteria except for the following single point: Fischer described direct linking of alanine to the 2-position of glycerol, whereas we detected its linkage to the glucose residue. These apparently almost identical conclusions, however, have completely different implications. Fischer's group had first studied the structure of major components of LTA regardless of their biological activities. In their later publications (*14*, *15*), the immunostimulating activity of the whole LTA was described again without separation. Such an approach might lead to the incorrect understanding that the chemical entities whose structures had been elucidated by them were responsible for the activity. By contrast, the present work has clearly demonstrated the chemical structure of the major component, which was proved to be inactive in the present test system of cytokine-inducing with human peripheral whole blood cells, of LTA from *E. hirae* ATCC 9790. This means that the immunostimulatory minor components in LTA (described in Chapter II) must be structurally distinct from the major component shown in Figure 3-10. In other words, the presence of unsaturated fatty acids, long chain poly(glycerophosphate), or glucose or alanine substituents on the glycerol as discussed in Chapter I, is irrelevant to the lack of cytokine-inducing activity of the previously synthesized fundamental structures of LTA (*1*, *2*, *4*).

The major component in BOS60 which is more lipophilic than BOS40 also lacked the cytokine-inducing activity (described in Chapter II). The chemical structure of this inactive component has not been fully studied, but its chemical structure is assumed at present to be identical to LTA-2 which has, as proposed by Fischer, an additional phosphatidyl substituent at the 6-position of the reducing side glucose of the glycolipid part of LTA-1 (*3*).

REFERENCES

1) Fukase, K., Matsumoto, T., Ito, N., Yoshimura, T., Kotani, S., and Kusumoto, S. (1992) *Bull. Chem. Soc. Jpn.* **65**, 2643-2654.

2) Fukase, K., Yoshimura, T., Kotani, S., and Kusumoto, S. (1994) *Bull. Chem. Soc. Jpn.* **67**, 473-482.

3) Fischer, W. (1990) in *Glycolipids, Phosphoglycolipids and Sulfoglycolipids* (Kates, M., ed.) pp. 123-234, Plenum Press, New York.

4) Takada, H., Kawabata, Y., Arakaki, R., Kusumoto, S., Fukase, K., Suda, Y., Yoshimura, T., Kokeguchi, S., Kato, K., Komuro, T., Tanaka, N., Saito, M., Yoshida, T., Sato, M., and Kotani, S. (1995) *Infect. Immun.* **63**, 57-65.

5) Suda, Y., Tochio, H., Kawano, K., Takada, H., Yoshida, T., Kotani, S., and Kusumoto, S. (1995) *FEMS Immunol. Med. Microbiol.* **12**, 97-112.

6) Ikemoto, S., Katoh, K., and Komagata, K. (1978) *J. Gen. Appl. Microbiol.* **24**, 41-49.

7) Torello, L.A., Yates, A.J., and Thompson, D.K. (1980) *J. Chromatography* **202**, 195-209.

8) Schagger, H. and Jagow, G.V. (1987) *Anal. Biochem.* **166**, 368-379.

9) Rice, K.G., Rottink, M.K.,and Linhardt, R.J. (1987) *Biochem. J.* **244**, 515-522.

10) Tsai, C.M. and Frasch, C.E. (1982) *Anal. Biochem.* **119**, 115-119

11) Kochanowski, B., Fischer, W., Iida-Tanaka, N., and Ishizuka, I. (1993) *Eur. J. Biochem.* **214**, 747-755.

12) Altona, C. and Haasnoot, C.A.G. (1980) *Org. Magn. Reson.* **13**, 417-429.

13) Dabrowski, J., Hanfland, P., and Egge H. (1982) *Methods Enzymol.* **83**, 69-86.

14) Bhakdi, S., Klonisch, T., Nuber, P. and Fischer, W. (1991) *Infect. Immun.* **59**, 4614-4620.

15) Keller, R., Fischer, W., Keist, R. and Bassetti, S. (1992) *Infect. Immun.* **60**, 3664-3672.

IV. Structural analysis of one of the cytokine-inducing components

Several research groups reported previously that LTA shared some biological activities with LPS (*1-4*). The activities includes the activation of macrophage and the stimulation of cytokine secretion. In those studies, the LTA fraction (such as LTA-1 and LTA-2 in *E. hirae*) extracted from bacterial cells was assumed as if it had consisted of homogeneous component of the structure proposed by Fischer (*5*), and that particular component had been responsible for the observed biological activities of the whole LTA fraction. The LTA fraction is, however, not homogeneous: that from *E. hirae* ATCC 9790 was separated into cytokine-inducing several minor components and an inactive major one as described in Chapter II. Kusunoki *et al.* (*6, 7*) also reported the occurrence and partial purification of a minor component, which induced cytokine production, from the LTA fraction of *Staphylococcus aureus*. The chemical structure of these cytokine-inducing components, however, was not elucidated yet. As described in Chapter III, the structure of the major component, which lacks the cytokine-inducing activity, coincides with the one proposed by Fischer (*5*) for an LTA isolated from the same species of bacteria.

The structural investigation of one of the cytokine-inducing components (OS-4L, Scheme 2-2) containing mannose is described in this chapter.

MATERIALS AND METHODS

Methylation analysis

Methylation analysis was performed according to the method of Ciucanu and Kereu (*8*). Test sample (100 μg) was dissolved in 0.5 ml of DMSO by sonication. Sodium hydroxide suspended in DMSO (0.2 ml, 100 mg/ml) and 0.1 ml of methyl iodide were added. The mixture was sonicated at room temperature in a sealed tube under nitrogen atmosphere for 20 min. After addition of 1 ml of water, permethylated products were extracted with 1 ml of chloroform. After washing twice with each 1 ml of water, the chloroform phase was concentrated *in vacuo* to dryness with a rotary evaporator.

The residue dissolved in 0.5 ml of 2 M TFA was heated at 125°C in a sealed tube under nitrogen atmosphere for 3 h. After evaporation of the solvent, the residue was dissolved in 0.5 ml of aqueous sodium borohydride (2 mg/ml) and allowed to stand at room temperature for 1 h. After addition of a few drops of acetic acid, the mixture was concentrated *in vacuo* to dryness. The residue was dissolved in 1 ml of methanol and then evaporated. This procedure was repeated total three times. The residue was dissolved in 0.5 ml of acetic anhydride-pyridine (1/1, v/v), heated at 100°C for 1 h, and concentrated *in vacuo*. The residue was partitioned with 0.5 ml of water and 0.5 ml of chloroform. The chloroform phase containing partially methylated alditol acetate was separated, washed three times with each 0.5 ml of water, and concentrated *in vacuo*. The residue was dissolved in 100 μl of acetone, and then 2 μl of the solution was analyzed by GC and GC-MS under similar conditions for carbohydrate analysis in Chapter III.

Reducing sugar analysis

An aqueous test sample solution (20 μl, 1 mg/ml), 20 μl of 0.3% aqueous pyridinium hydrogen 3,6-dinitrophthalate, and 25 μl of an aqueous solution containing of potassium carbonate (25%) and sodium thiosulfate (5%) were placed in a 1.5 ml polypropylene tube and

heated at 100°C for 10 min. After cooling to room temperature, the absorbance at 450 nm was measured. Calibration was performed by using glucose.

TLC and other analysis

TLC was performed as the method described in Chapter III using solvent system C: chloroform/acetone (5/1, v/v). Phosphorus, fatty acids, carbohydrate, glycerol, and amino acids were analyzed according to the method described in Chapter III. SDS-PAGE and HPLC were also performed as described in Chapter III. Proton and ^{13}C NMR spectra were measured in a way similar to that described in Chapter III. Proton NMR spectra were measured on a UNITY plus spectrometer (Varian, Palo Alto, CA, USA) at 600 MHz and a UNITY INOVA spectrometer (Varian) at 750 MHz. FAB-, ESI-, and MALDI-TOF-MS were obtained by the method described in Chapter III. Determination of phosphomonoester in OS-4L was done with the procedure in Chapter III.

Deacylation

Deacylation of OS-4L (1.6 mg) was performed according to the procedure described in Chapter III.

Hydrolysis with 47% hydrofluoric acid

Hydrolysis of OS-4L (3 mg) with 47% hydrofluoric acid and phase partition of the reaction products was performed with the procedure described in Chapter III. The products extracted in the aqueous phase were fractionated on a Sephadex G-100 column (1.5 x 95 cm, Pharmacia). According to the elution profile, three fractions (abbreviated as G100-I, -II and -III) were obtained, concentrated in vacuo with a rotary evaporator, and lyophilized.

Acetolysis

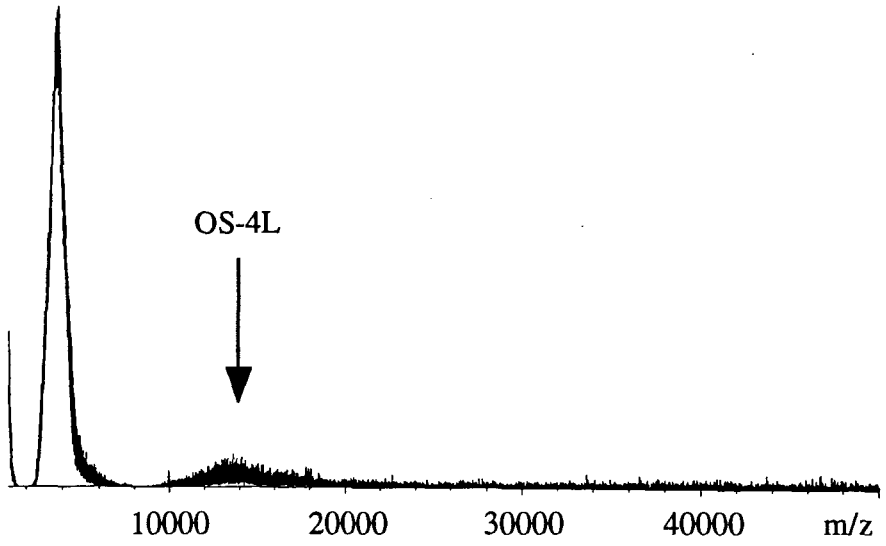

Figure 4-1. MALDI-TOF-MS analysis of OS-4L with Kompact MALDI IV in the linear and positive mode. 2,5-Dihydroxybenzoic acid was used as a matrix. The peak at *ca.* 4000 arises from the matrix.

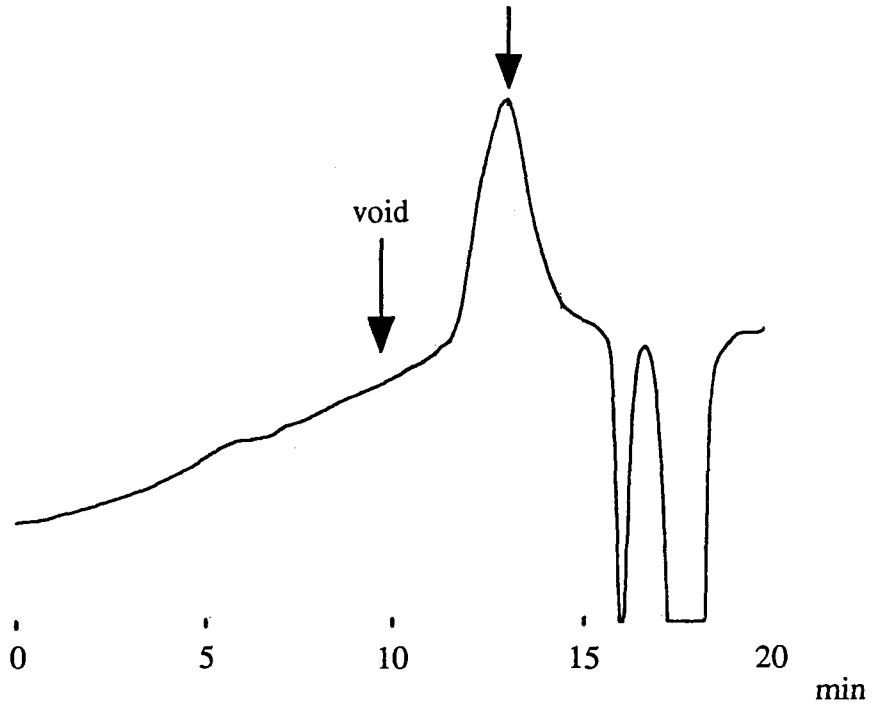

Figure 4-2. The elution profile of the deacylated OS-4L on gel permeation HPLC. The troughs after 16 min are due to turbulence by the solvent.

Acetolysis was performed according to the method of Shibata (*10*) with a slight modification. G100-I (0.2 mg) was dissolved in 5 μl of formamide by sonication. After addition of 5 μl of pyridine and 5 μl of acetic anhydride, the mixture was heated at 40°C for 12 h. After addition of 0.5 ml of water, the reaction mixture was centrifuged at 1000 x g for 5 min. The precipitate was separated, washed twice with each 0.5 ml of water, and dried *in vacuo*. The precipitate was dissolved in 25 μl of a mixture of acetic acid, acetic anhydride, and sulfuric acid (100/100/1, v/v/v) and heated at 40°C for 12 h. The reaction mixture was partitioned with 0.5 ml of water and 0.5 ml of chloroform. The chloroform phase was separated, washed five times with each 0.5 ml of water, and concentrated *in vacuo* to dryness with a rotary evaporator. The products were separated by TLC using solvent system C.

Preparation of standard peracetylated oligomannosides

Acetolysis of the commercially available mannan (from *Saccharomyces cerevisiae*, Sigma) and separation of the products by TLC were performed by the procedure described above.

RESULTS AND DISCUSSION

The chemical structure of OS-4L, which was the main member among the cytokine-inducing components from the LTA fraction, was studied. The molecular weight of OS-4L was analyzed by MALDI-TOF-MS. In the linear and positive mode, a broad peak in the range of 1.0-1.9 x 10^4 (the peak top at 1.4 x 10^4) was observed (Figure 4-1). In contrast, no clear band was visualized in SDS-PAGE analysis either by periodate oxidation followed by silver staining or Alcian blue staining. In spite of the failure in observing a definite peak in HPLC analysis of OS-4L itself owing probably to mutual aggregation, deacylated OS-4L was eluted

Table 4-1. Chemical compositions of OS-4L.

	μmol / mg		Molar ratio [a),b)]	
Phosphate	0.61		1.0	(10.8)
Sugars	3.44			
Man		2.89	4.8	(50.9)
Glc		0.55	0.90	(9.5)
Fatty acids	0.36			
14:0		0.02	0.02	(0.3)
16:0		0.14	0.24	(2.5)
16:1		0.03	0.05	(0.6)
18:0		0.03	0.05	(0.5)
18:1		0.14	0.24	(2.5)
Glycerol	0.77		1.3	(13.4)
Amino acids	0.30			
Asp		0.03	0.09	(0.9)
Thr		0.02	0.05	(0.6)
Ser		0.07	0.17	(1.8)
Glu		0.03	0.07	(0.8)
Gly		0.05	0.12	(1.3)
Ala		0.08	0.20	(2.1)

a) Molar ratios were calculated by assuming the presence of one mole of phosphate.
b) The values in the parentheses represent the numbers of respective residues as calculated by assuming the molecular weight of OS-4L as 1.4×10^4.

Table 4-2. Methylation analysis of OS-4L and G100-I.

	Molar ratio [a)]	
	OS-4L	G100-I
O-substituted mannose		
non-	1.00	1.00
2-	0.86	0.84
3-	b)	b)
6-	b)	b)
2,6-di-	1.28	1.38
non-substituted glucose	0.21	0.12

a) Molar ratio was estimated from the peak areas in GC analysis.
b) Quantitative analysis failed because of overlapping of peaks due to unknown minor components

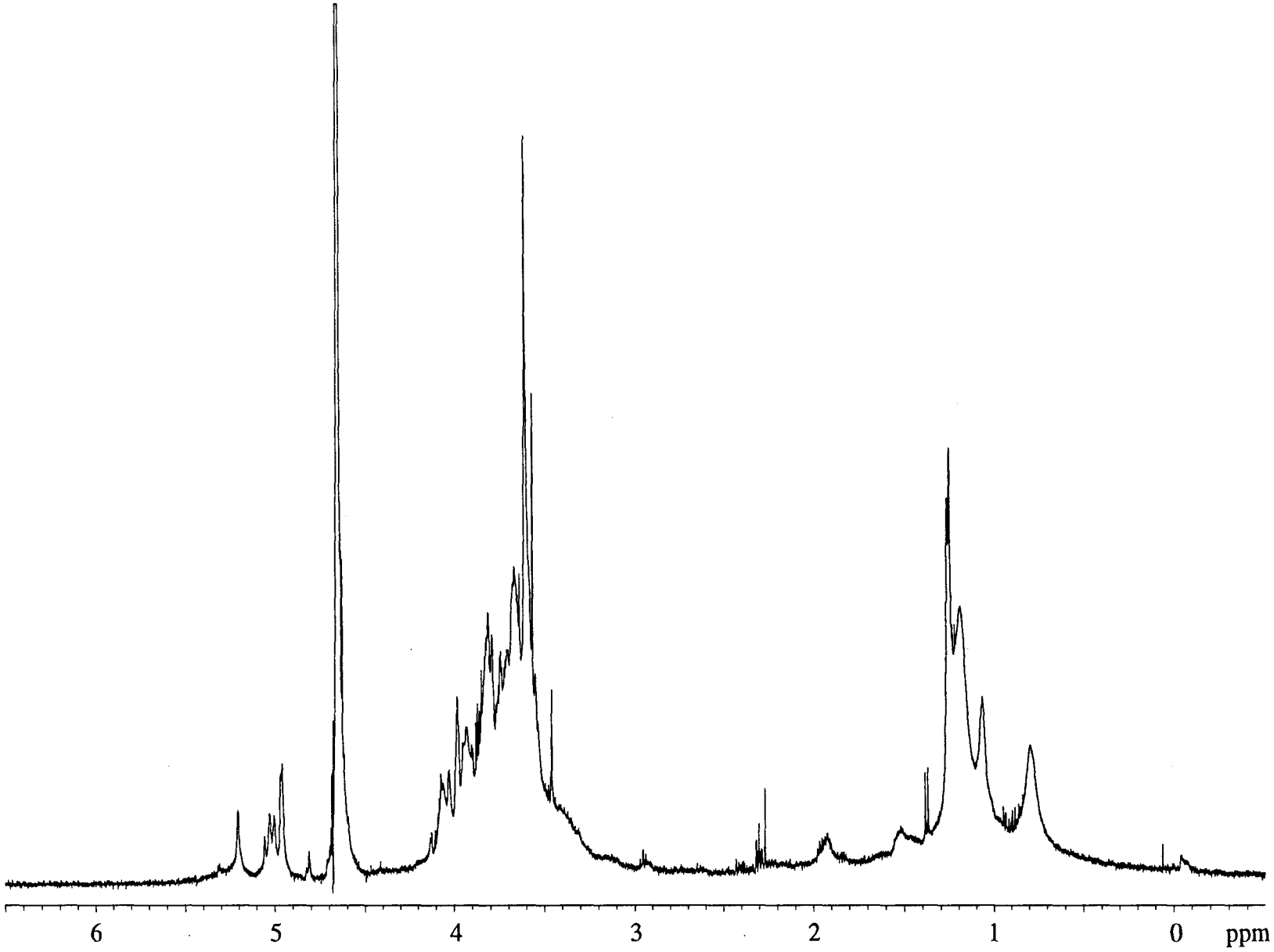

Figure 4-3. ^{1}H MNR spectrum of OS-4L. The spectrum was measured in D_2O at 303K.

Scheme 4-1. The degradation procedure of OS-4L.

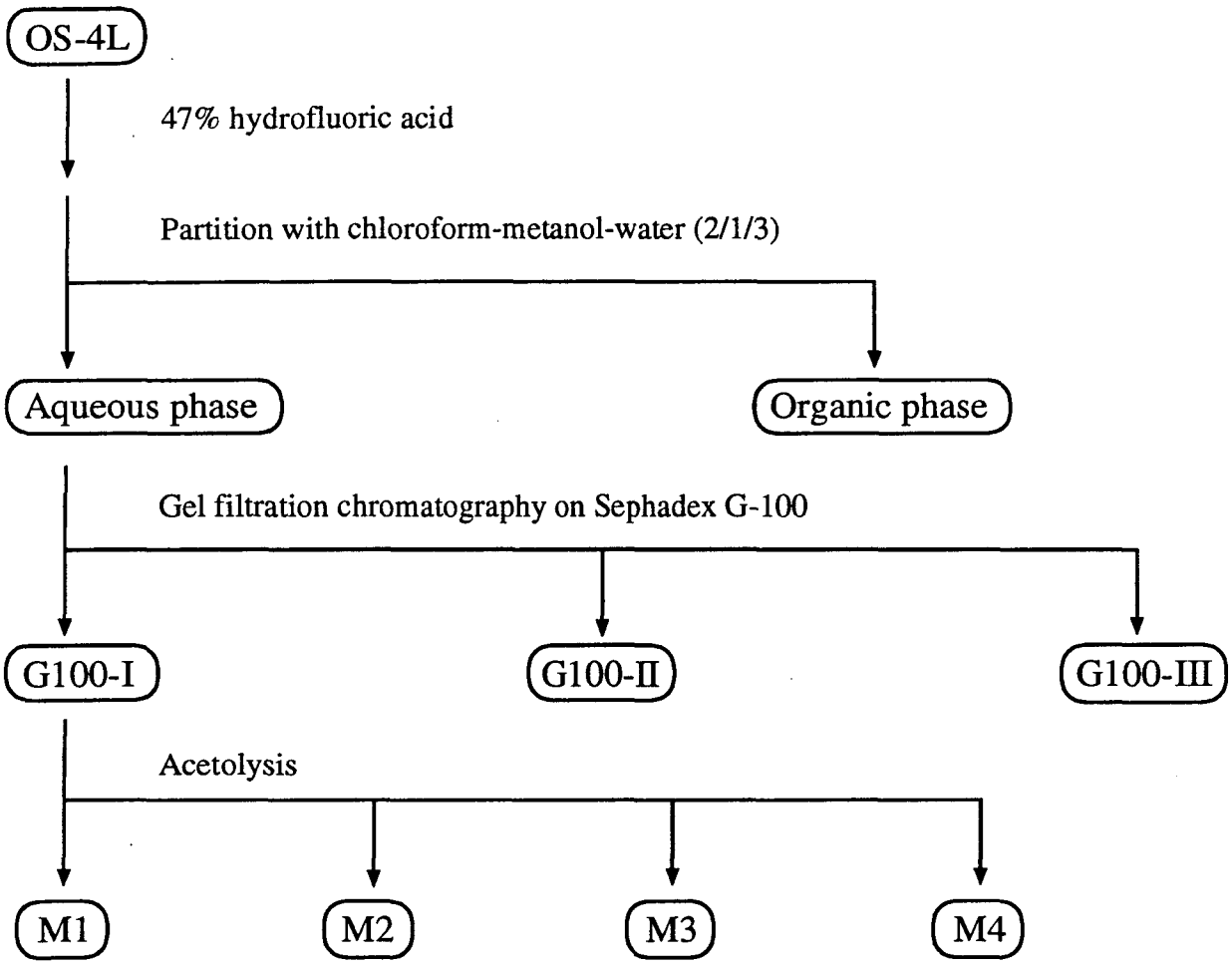

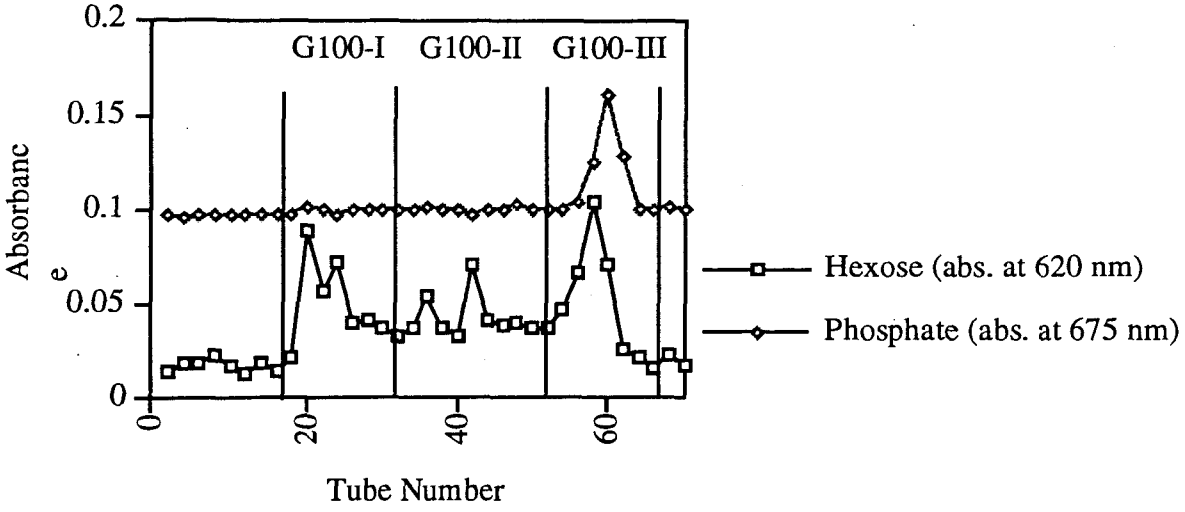

Figure 4-4. The elution profile of the products extracted in the aqueous phase from the HF-hydrolysate of OS-4L on Sephadex G-100.

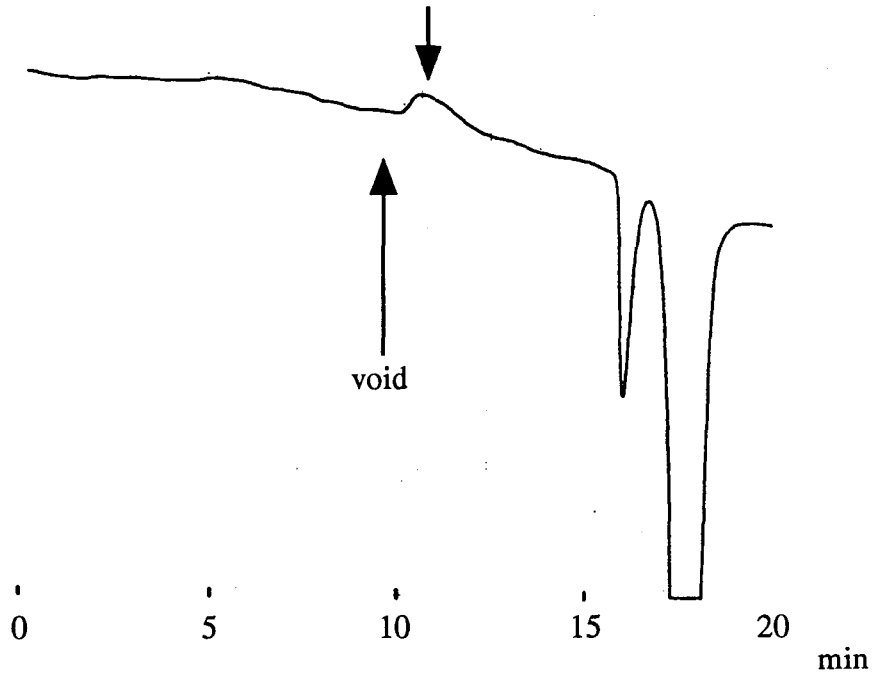

Figure 4-5. The elution profile of G100-I on gel permeation HPLC. The troughs after 16 min are due to turbulence by the solvent.

as a broad but single peak in gel permeation HPLC (Figure 4-2). OS-4L can therefore be regarded as a single macromolecular glycoconjugate with the above-mentioned molecular weight range due to the presence of homologues.

The chemical compositions of OS-4L are summarized in Table 4-1. OS-4L consists of phosphate, carbohydrates, fatty acids, glycerol, and amino acids. The molar ratios estimated by assuming the molecular weight of OS-4L to be 1.4×10^4 are also summarized in Table 4-1. Since no free phosphate was liberated by direct alkaline phosphatase digestion of OS-4L, the presence of phosphomonoester was excluded. Carbohydrates consisted of mannose and glucose (molar ratio was 5.3:1.0). On methylation analysis (Table 4-2), the mannose residues were mainly characterized as non-substituted, 2-*O*-substituted, and 2,6-di-*O*-substituted mannose. 3-*O*-Substituted and 6-*O*-substituted mannose residues were also detected but in much lower amounts. Glucose was detected only as non-substituted form and substituted glucose was not detected at all. No reducing sugar was detected. Fatty acids were mainly hexadecanoic acid octadecenoic acid. Several amino acids were also detected, suggesting the possible presence of a covalently bound oligopeptide.

Proton NMR spectrum of OS-4L is shown in Figure 4-3. Because of the broad signals due to the high molecular weight of the substrate and their overlapping, only partial assignment of signals was possible. Thus, the molecular size was reduced as shown in Scheme 4-1. OS-4L was first hydrolyzed with 47% hydrofluoric acid (HF) which was expected to cleave off the moieties bound *via* phosphodiester linkages. The ^{1}H NMR spectrum of the products which were extracted into the aqueous phase from the HF-hydrolysate indicated that fatty acids were almost removed, suggesting that the lipophilic part containing fatty acids was bound to the hydrophilic region in OS-4L via phosphodiester linkages. The hydrophilic products were further separated by gel filtration chromatography on Sephadex G-100 into three fractions, G100-I, -II, and -III (Figure 4-4).

G100-I was eluted as a broad peak in gel permeation HPLC (Figure 4-5) and the

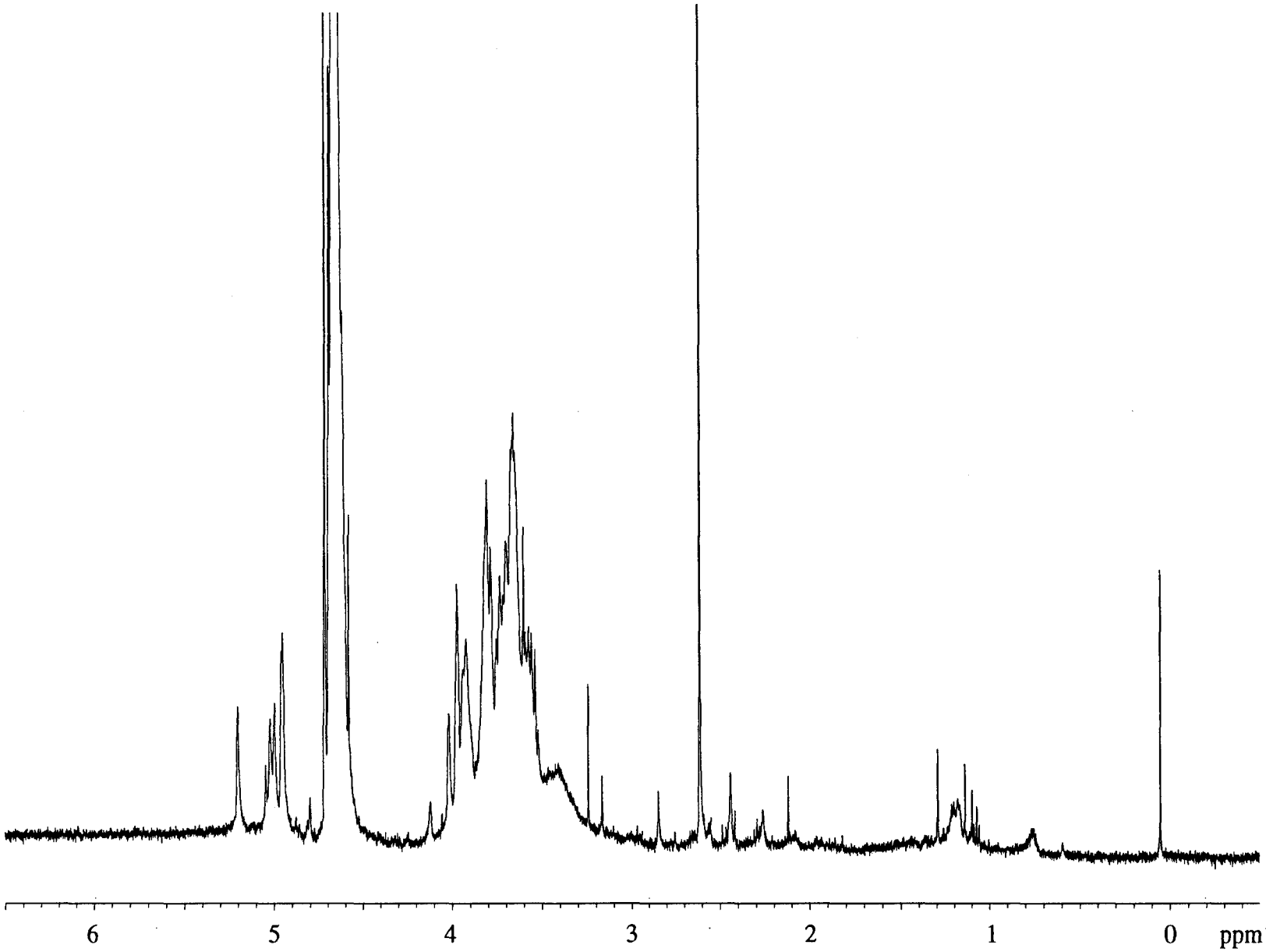

Figure 4-6. ^{1}H MNR spectrum of G100-I. The spectrum was measured in D_2O at 303K.

Table 4-3. Chemical compositions of G100-I and G100-III.

	μmol / mg	
	G100-I	G100-III
phosphate	0	1.2
Mannose	1.1	0
Glucose	0.18	0.1
glycerol	0	1.2

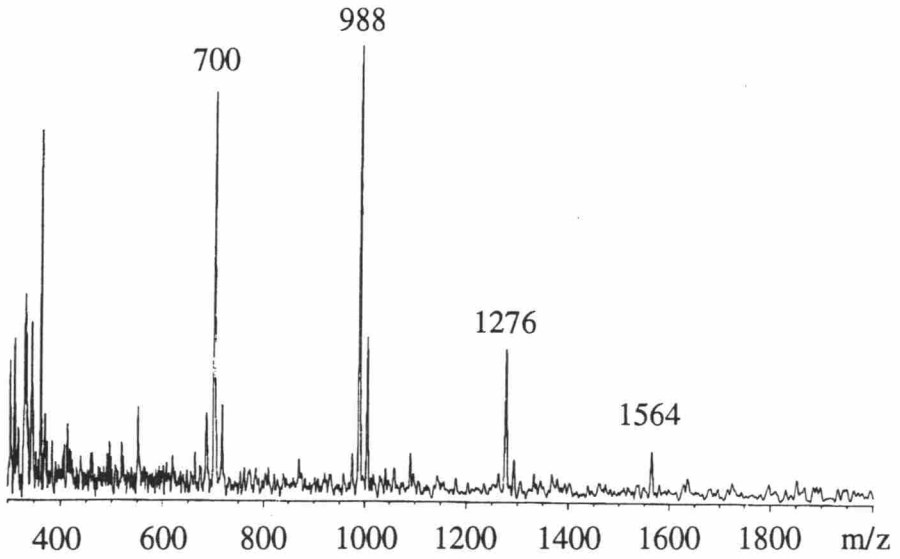

Figure 4-7. MALDI-TOF-MS analysis of acetolysis products from G100-I in the refrectron and positive mode. 2,5-Dihydroxybenzoic acid was used as a matrix.

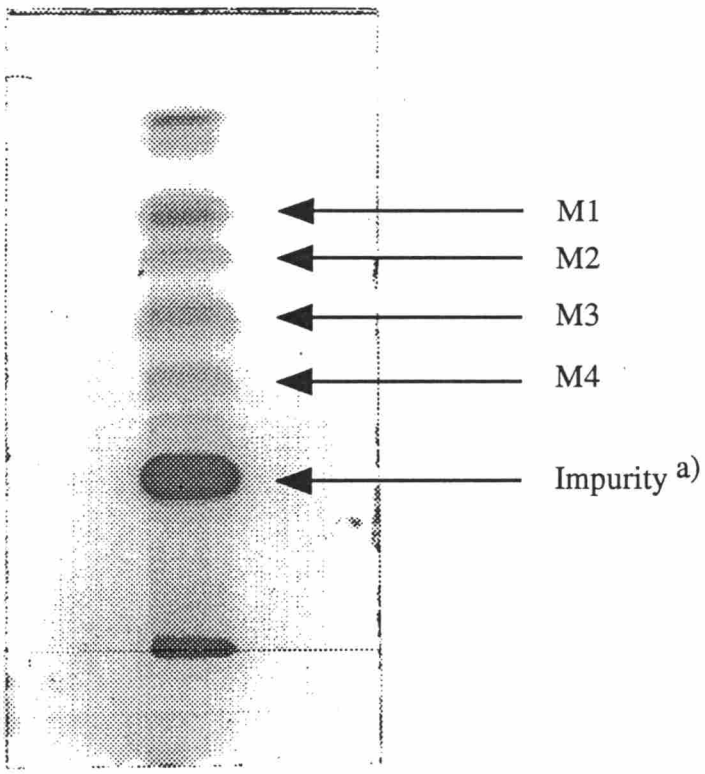

Figure 4-8. A TLC profile of the acetolysis products from G100-I. TLC was done on a silica gel plate (Merck Keiselgel 60 F_{254} Art. 5715) using solvent system C: chloroform-acetone (5/1, v/v). The products were visualized with iodine vapor.
a) derived from polypropylene tube.

Table 4-4. ^{1}H NMR data for the acetolysis products from G100-I. The spectra of M2 and M3 were measured at 500 MHz in $CDCl_3$ at 303K. The spectra of M4 were measured at 600 MHz or 750 MHz in $CDCl_3$ at 303K. The assignments were established by ^{1}H one-dimensional spectroscopy, one-dimensional NOE spectroscopy, and two-dimensional methods, COSY and NOESY. Mannose residues are numbered from the reducing terminus to the non-reducing terminus.

Proton	Chemical shift δ (Coupling constants) (Hz)		
	M2	M3	M4
Man^{I} H-1	6.23 (2.1)	6.23 (1.8)	6.25 (1.9)
Man^{I} H-2	4.03 (2.3, 3.2)	4.06	4.05
Man^{I} H-3	5.28 (3.1, 10.2)	5.30	5.32
Man^{I} H-4	5.42 (10.3, 10.1)	nd	nd
Man^{I} H-5	3.99	nd	nd
Man^{I} H-6	4.22 (4.1, 12.4) 4.12 (2.3, 12.1)	nd	nd
Man^{II} H-1	4.94 (2.1)	5.11 (2.1)	5.11 (1.6)
Man^{II} H-2	5.25	4.11	4.11
Man^{II} H-3	5.39 (3.2, 10.0)	5.29	nd
Man^{II} H-4	5.25	nd	nd
Man^{II} H-5	4.17	nd	nd
Man^{II} H-6a	nd	nd	nd
Man^{III} H-1		4.94 (1.9)	4.94 (1.9)
Man^{III} H-2		5.27	5.23
Man^{III} H-3		nd	4.14
Man^{III} H-4		nd	nd
Man^{III} H-5		nd	nd
Man^{III} H-6		nd	nd
Man^{IV} H-1			5.04 (1.9)
Man^{IV} H-2			5.07 (1.9, 3.6)
Man^{IV} H-3			nd
Man^{IV} H-4			nd
Man^{IV} H-5			nd
Man^{IV} H-6			nd nd

nd: not determined because of signal overlapping.

Table 4-5. ^{1}H NMR data for the standard peracetylated oligomannose, peracetylated Man(α1-2)Man, Man(α1-2)Man(α1-2)Man, and Man(α1-3)Man(α1-2)Man(α1-2)Man. The spectra were measured at 500 MHz in $CDCl_3$ at 303K. The assignments were established by ^{1}H and ^{13}C one-dimensional spectroscopy, ^{13}C DEPT, and following two-dimensional methods: COSY, NOESY, HMQC, and HMBC. Mannose residues are numbered from the reducing terminus to the non-reducing terminus.

Proton	Chemical shift δ (Coupling constants) (Hz)		
	Man(α1-2)Man	Man(α1-2)Man(α1-2)Man	Man(α1-3)Man(α1-2)Man(α1-2)Man
Man^{I} H-1	6.22 (2.3)	6.22 (2.1)	6.23 (2.3)
Man^{I} H-2	4.03 (2.3, 3.0)	4.05 (2.7)	4.04 (2.7, 5.5)
Man^{I} H-3	5.28 (3.2, 10.1)	5.30	5.29
Man^{I} H-4	5.41 (10.3, 10.0)	5.37 (9.6, 9.6)	5.38 (9.8, 9.9)
Man^{I} H-5	3.99 (2.3, 3.7, 10.0)	4.00	4.00
Man^{I} H-6	4.22 (3.9, 12.6)	4.22 (4.2, 12.6)	4.22 (4.0, 12.4)
	4.11 (2.4, 12.4)	4.10	4.10
Man^{II} H-1	4.93 (1.8)	5.11 (2.1)	5.09 (1.8)
Man^{II} H-2	5.25	4.11	4.09
Man^{II} H-3	5.39 (3.4, 10.0)	5.30	5.30
Man^{II} H-4	5.25	5.30	5.21 (9.9, 10.0)
Man^{II} H-5	4.17	4.10	4.11
Man^{II} H-6a	nd	nd	4.12
Man^{III} H-1		4.92 (1.8)	4.92 (1.8)
Man^{III} H-2		5.25 (1.9, 3.5)	5.22 (1.6, 3.8)
Man^{III} H-3		5.36 (10.1)	4.15
Man^{III} H-4		5.26 (10.0, 10.1)	5.28 (9.6, 9.7)
Man^{III} H-5		4.10	4.15
Man^{III} H-6		nd	4.18
Man^{IV} H-1			5.01 (1.6)
Man^{IV} H-2			5.05 (1.8, 3.5)
Man^{IV} H-3			5.19 (3.4, 10.0)
Man^{IV} H-4			5.31 (9.9, 10.0)
Man^{IV} H-5			4.00
Man^{IV} H-6			4.29 (4.0, 12.3)
			4.03

nd: not determined because of signal overlapping.

attempt to determine the molecular weight of G100-I by MALDI-TOF-MS was not successful. From ^{1}H NMR spectrum showed in Figure 4-6, the signals of the anomeric protons of the carbohydrate moieties in G100-I were almost identical to those of OS-4L, suggesting that the carbohydrate part in OS-4L was not influenced by the HF treatment. The chemical composition analysis of G100-I (Table 4-3) showed that it contains mannose and glucose (molar ratio was 6.3:1.0), but not phosphate and glycerol. From the methylation analysis (Table 4-2), the mannose residues in G100-I are mainly in non-substituted, 2-*O*-substituted, and 2,6-di-*O*-substituted forms.

To analyze the structure of G100-I in more details, it was subjected to acetolysis according to the method of Shibata *et al.* (*10*). A commercially available mannan from *Saccharomyces cerevisiae* was first treated by this method to evaluate the selectivity of the preferential cleavage of 1-6 linkages and to prepare standard oligosaccharides of mannose. Peracetylated Man, Man(α1-2)Man, Man(α1-2)Man(α1-2)Man, and Man(α1-3)Man(α1-2)Man(α1-2)Man were obtained in good yields as described (*11*). In the all oligomannosides isolated, no Man(1-6)Man linkage was retained: the highly selective cleavage of Man(1-6)Man linkage was confirmed under the conditions of acetolysis employed. Then G100-I was subjected to acetolysis under the same conditions and the products were analyzed by MALDI-TOF-MS (Figure 4-7). In the reflectron and positive mode, distinct ion peaks at m/z 700, 988, 1276, and 1564 were observed. These were assigned to the sodium adduct ions of peracetylated Hex_n (n=2-5). Then the products were separated by TLC using solvent system C (Figure 4-8). Four major products (abbreviated as M1, M2, M3, and M4) containing only mannose were then characterized on the basis of their ^{1}H-NMR data (Table 4-4) in comparison with those of the standard compounds (Table 4-5) and FAB-MS as described bellow. Analysis of other bands in TLC were not possible because of their low yields.

M1 was characterized as peracetylated mannose by ^{1}H NMR spectra. In the positive mode FAB-MS analysis of M2, an ion peak at m/z 701 was observed, indicating the sodium

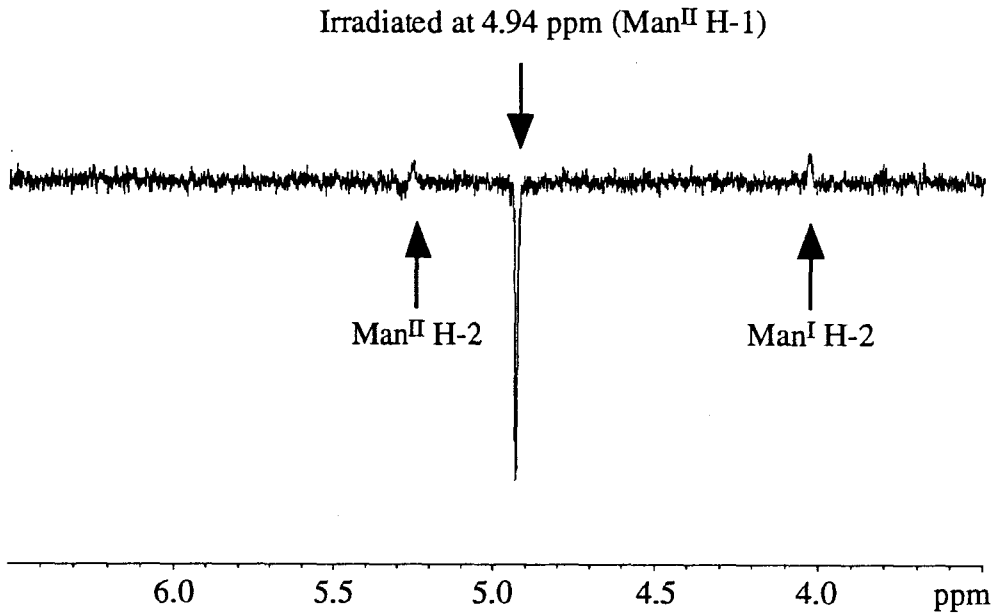

Figure 4-9. A part of NOE spectrum of M2. The spectrum was measured in $CDCl_3$ at 303K

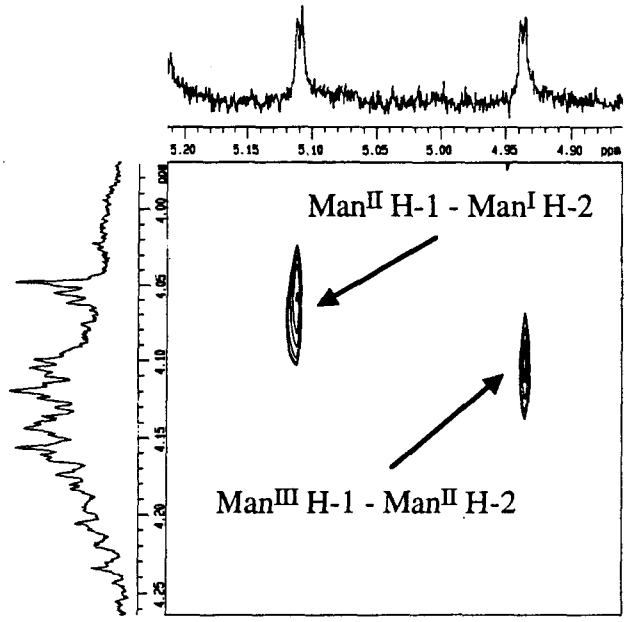

Figure 4-10. A part of NOESY spectrum of M3. The spectrum was measured in $CDCl_3$ at 303K. The mixing time was 650 ms.

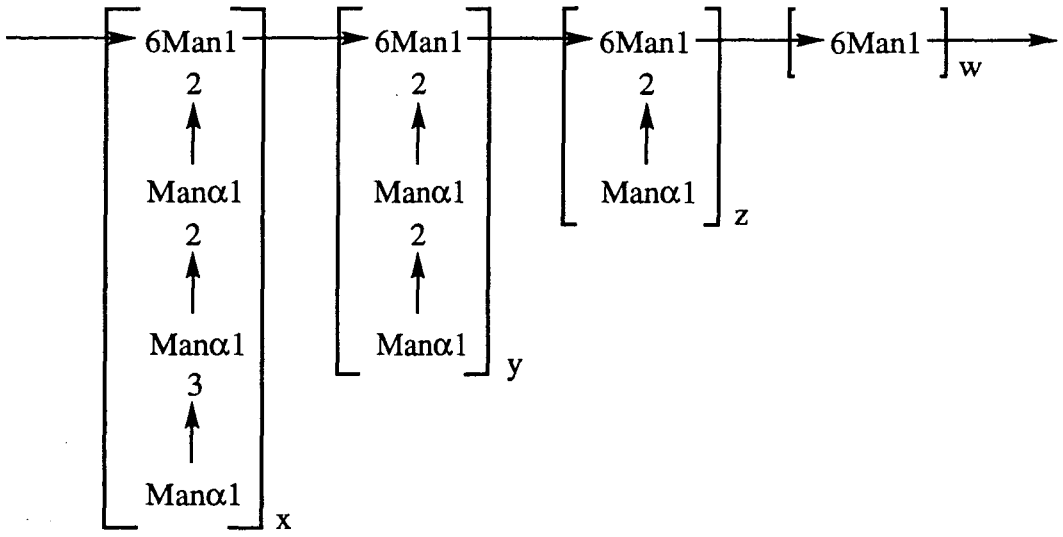

Figure 4-11. A major structure of mannose-rich region in G100-I. x:y:z:w = 1:7:4:1. The sequence of each substructure is interchangeable.

adduct ion of peracetylated Man_2. No downfield shifts of Man^{I} H-2 and Man^{II} H-1 in M2 were observed in the ^1H NMR spectra, indicating the Man^{II}(1-2)Man^{I} linkage. The interresidual linkage was confirmed by one dimensional NOE spectra (Figure 4-9), in which an interresidual correlation between Man^{II} H-1 and Man^{I} H-2 was observed. An ion peak at m/z 989 found in M3 corresponds to the sodium adduct ion of peracetylated Man_3. No downfield shifts of Man^{I} H-2, Man^{II} H-2, Man^{II} H-1, and Man^{III} H-1, and interresidual correlations between Man^{II} H-1 and Man^{I} H-2, and Man^{III} H-1 and Man^{II} H-2 in NOESY spectra (Figure 4-10) showed the Man^{III}(1-2)Man^{II}(1-2)Man^{I} sequence. An ion peak at m/z 1277 found in M4 coincides with the mass number of the sodium adduct of peracetylated tetramannoside. No downfield shifts of three Man H-1, two Man H-2, and one Man H-3 were observed, indicating two Man(1-2)Man linkages and Man(1-3)Man linkage. The complete mannose sequence of M4, however, was not determined.

The ^1H NMR signals of the acetolysis products from G100-I was only partially assigned because the signals were overlapping and ^{13}C NMR measurement was impossible due to their low quantity, whereas that of standard authentic compounds prepared from *S. cerevisiae* was almost fully assigned by using DEPT, HMQC, and HMBC techniques (Table 4-5). To determine the mode of linkage and anomeric configurations of mannose residues in G100-I, ^1H NMR spectra of its acetolysis products were directly compared with those of standard compounds. M2, M3, and M4 were proved to be identical with peracetylated Man(α1-2)Man, Man(α1-2)Man(α1-2)Man, and Man(α1-3)Man(α1-2)Man(α1-2)Man, respectively. Since the present acetolysis reaction cleaves mainly Man(1-6)Man linkage, the oligomannosides (M1, M2, M3, and M4) are reasonably expected to have been connected to each other via Man(1-6)Man linkages. A plausible structure of the mannose-rich region in G100-I was therefore deduced as shown in Figure 4-11. The number of repeating unit (n, in Figure 4-11) was estimated to be 1-3 by assuming the molecular weight of OS-4L. The molar ratio of each sub unit (x,y,z, and w) was calculated from the peak area of H-1 in ^1H NMR of

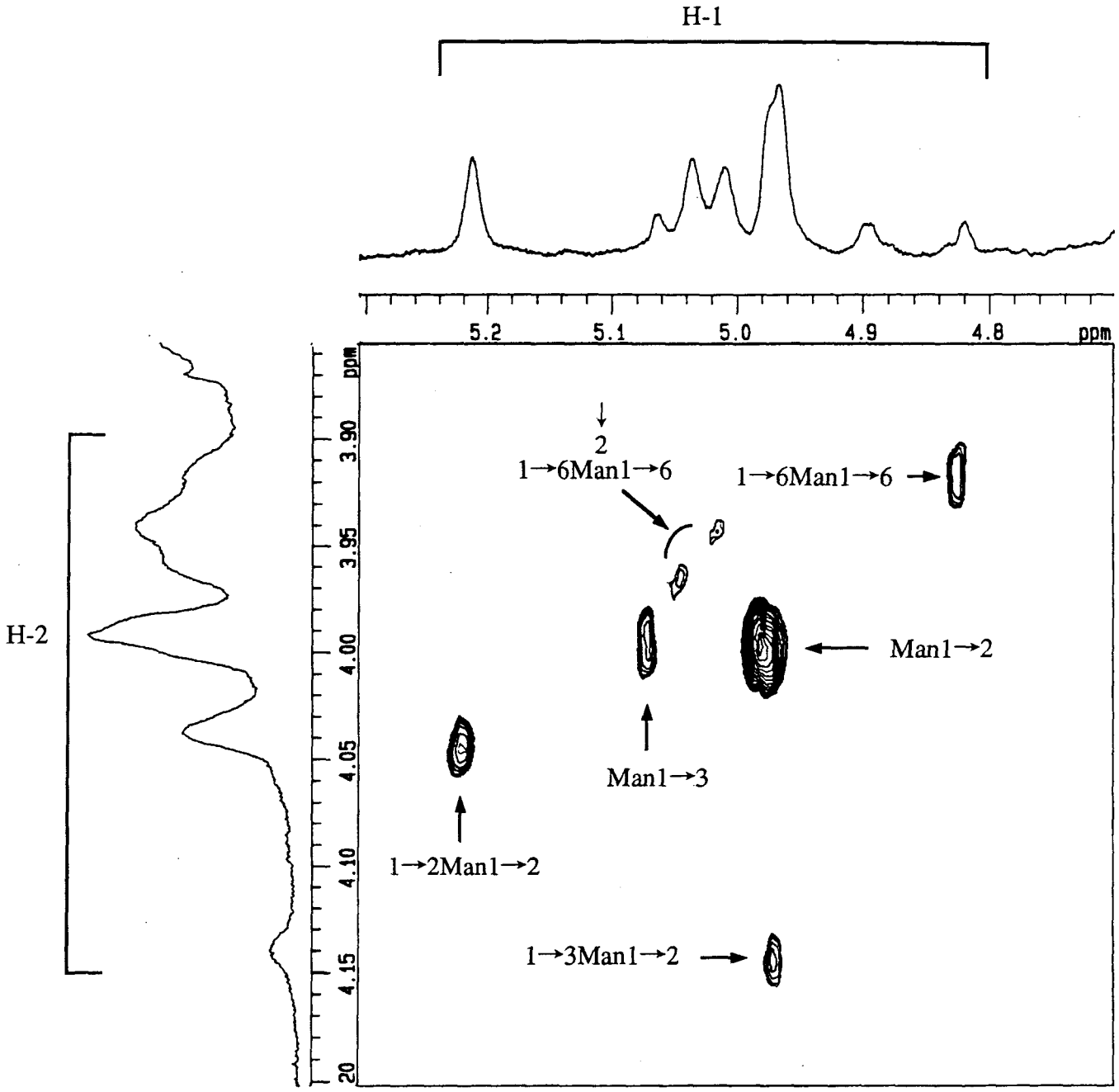

Figure 4-12. A part of COSY spectra of G100-I.

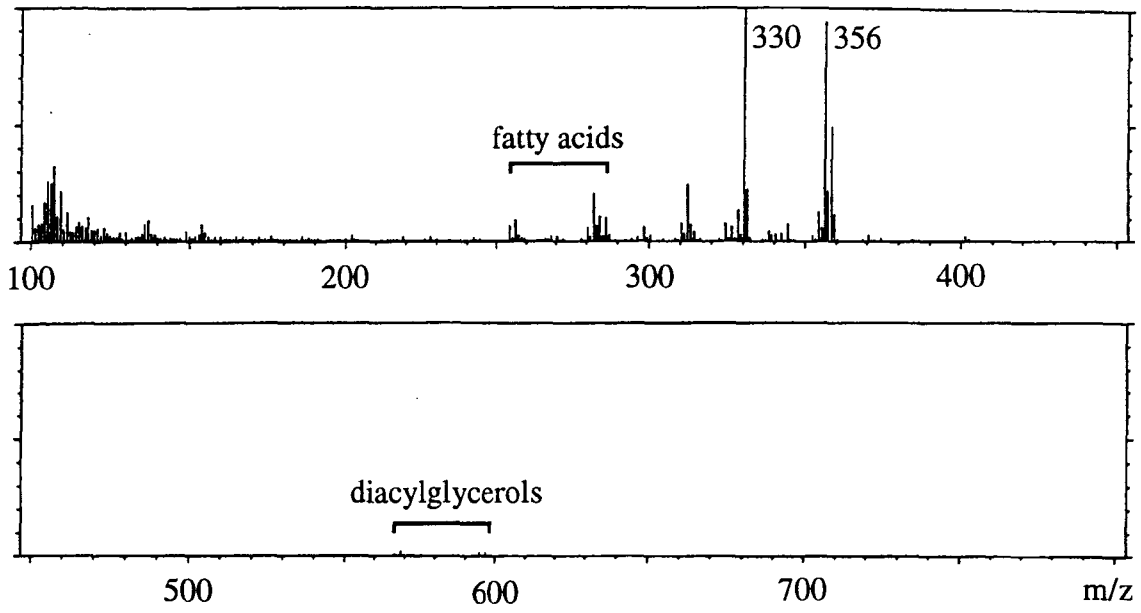

Figure 4-13. FAB-MS analysis of the products extracted in the organic phase from the HF-hydrolysate of OS-4L in positive mode. m-Nitrobenzyl alcohol was used as a matrix.

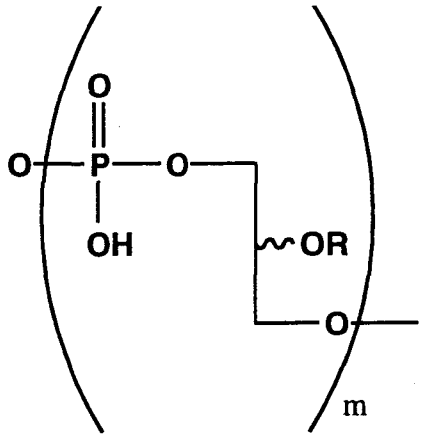

R = H,
hexadecanoyl,
octadecenoyl, etc.

Figure 4-14. A proposed structure of HF-liberated moiety from OS-4L.

G100-I (Figure 4-12). In the case of overlapping H-1 signals (δ around 4.96-4.99), their intensities were estimated from the intensities of respective H-2 signals. The assignments of correlations of each mannose units were established by reference to the data (*13*). The location of the minor glucose substitution, however, was not determined yet.

Proton NMR spectrum of G100-II was almost identical to those of G100-I, suggesting their same structural principle except for the molecular weight.

G100-III was eluted at near the bed volume of the Sephadex G-100 column, suggesting the presence of low molecular weight (less than 10^3) compounds. In chemical composition analysis of G100-III (Table 4-3), phosphate, glycerol, and trace amount of glucose were detected, but mannose was not. These data suggested the presence of glycerophosphate structure in OS-4L.

By the positive mode FAB-MS analysis of the products extracted in the organic phase from the HF-hydrolysate (Figure 4-13), acylglycerols were detected as main constituents: *e.g.*, the ion peaks at m/z 330 and 356 correspond to glyceryl hexadecanoate and glyceryl octadecenoate, respectively. The presence of small amount of fatty acids and trace amount of diacylglycerols was also observed. But no glycolipid was detected. Since the diacylglycerol was obtained by similar HF hydrolysis described in Chapter III, it can be concluded that no diacylglycerol but monoacylglycerol unit was originally present in OS-4L. The determination of the original position of the acyl substitution was not possible because acyl migration during HF hydrolysis could not be excluded.

The ratio of the methylated mannose derivatives obtained on methylation analysis of OS-4L was similar to those of G100-I (Table 4-2), which indicated that the number of the glycerophosphate moieties connected to G100-I is very low. Therefore, the liberated phosphate, glycerol, and acylglycerol on HF hydrolysis may construct the poly(glycerophosphate) structure (Figure 4-14).

From all the data presented above, OS-4L is concluded to consist of a mannose-rich

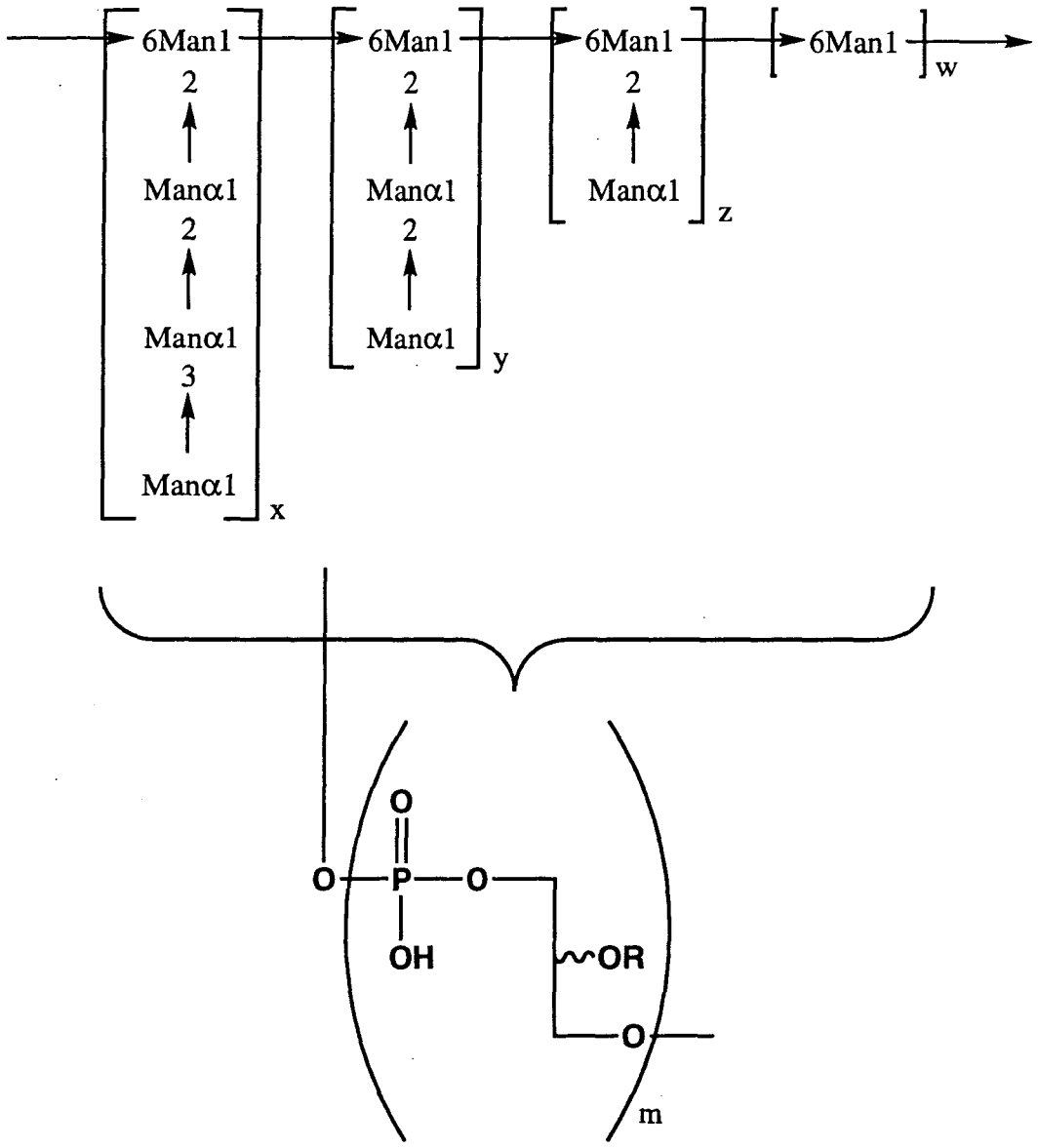

Figure 4-15. A fundamental structure proposed for a immunostimulating minor component, OS-4L, from the LTA fraction of *E. hirae* ATCC 9790.

highly branching polysaccharide backbone and lipophilic moieties which consists of glycerol and acylglycerol, the later being covalently bound to the former by phosphodiester linkage. A fundamental structure proposed for OS-4L is shown in Figure 4-15. The core structure responsible for its cytokine-inducing activity, however, is not clear. Garner *et al.* (*12*) reported that mannan from the cell wall of *Candida albicans* stimulates the production of TNF-α by macrophage. Chatterjee *et al.* (*13*) and Suda *et al.* (*14*) reported that mannose containing glycoconjugates from several mycobacteria induce IL-6 and TNF-α. These observations show that the oligomannoside moiety may play an important role for stimulation of cytokine production. The outer chain polysaccharide in *Saccharomyces cerevisiae* mannan whose structure is close to that of the major polysaccharide part in OS-4L was, however, inactive in the present test system for IL-6 induction. This may suggested that not only mannose moiety but also other components, such as lipophilic moiety or phosphate, is important for the activity. In agreement with this conclusion, the importance of lipophilic moiety was recently reported for several immunostimulating glycoconjugates (*8*, *15*).

REFERENCES

1) Bhakdi, S., Klonisch, T., Nuber, P. and Fischer, W. (1991) *Infect. Immun.* **59**, 4614-4620.

2) Keller, R., Fischer, W., Keist, R. and Bassetti, S. (1992) *Infect. Immun.* **60**, 3664-3672.

3) Renzi, P.M., and Lee, C-H. (1995) *J. Endotoxin Res.* **2**, 431-441.

4) Cleveland, M.G., Gorham, J.D., Murphy, T.L., Toumanen, E., and Murphy, K.M. (1996) *Infect. Immun.* **64**, 1906-1912.

5) Fischer, W. (1990) in *Glycolipids, Phosphoglycolipids and Sulfoglycolipids* (Kates, M., ed.) pp. 123-234, Plenum Press, New York

6) Kusunoki, T., Hailman, E., Juan, T.S.-C., Lichenstein, H.S., Wright, S.D. (1995) *J. Exp. Med.* **182**, 1673-1682

7) Kusunoki, T. and Wright, S.D. (1996) *J. Immunol.* **157**, 5112-5117

8) Ciucanu, I. and Kerek, F. (1984) *Carbohydr. Res.* **131**, 209-217

9) Momose, T. (1972) in *Yuuki teisei bunseki* pp.226, Hirokawa, Tokyo.

10) Shibata, N., Kojima, C., Satoh, Y., Suzuki, A., Kobayashi, H., and Suzuki, S. (1993) *Eur. J. Biochem.* **217**, 1-12

11) Lee, Y-C. and Ballou, C.E. (1965) *Biochemistry* **4**, 257-264.

12) Garner, R.E., Rubanowice, K., Sawyer, R.T., and Hudson, J.A. (1994) *J. Leukoc. Biol.* **55**, 161-168.

13) Chatterjee, D., Lowell, K., Rivoire, B., McNeil, R.M., and Brennan P.J. (1992) *J. Biol. Chem.* **267**, 6234.

14) Suda, Y., Hashimoto, M., Yasuoka, J-i., Okabe, E., Kusumoto, S., Takada, H., Hayashi, T., Tamura, T., and Kotani, S. (1996) *Polymer Preprints*, **37**, 129-130.

15) Okabe, E., Kawano, K., Suda, Y., Kusumoto, S., Hayashi, K., Aoyama, K., Tamura, T., and Kotani, S., "69th National Meeting of the Japanese Biochemical Society" Sapporo, August 1996, Abstr., No. 1-P-0060.

Summary

Chemical studies on glycoconjugates in the lipoteichoic acid fraction of *Enterococcus hirae* ATCC 9790 in relation to its immunobiological activity are described in this dissertation.

Rapid and efficient separation of the cytokine-inducing components of lipoteichoic acid fraction in a large scale was achieved by application of batch-wise and stepwise elution technique. A total of 46 mg of the active components were separated from *ca.* 1 kg of dried bacterial cells. (Chapter II)

The structure of the glycoconjugate obtained as the major but not cytokine-inducing component of LTA fraction was studied. Phosphodiester linkages present were cleaved by hydrofluoric acid hydrolysis and the hydrolysis products were separated and characterized by means of NMR and MS. The location of the phosphodiesters in the original glycoconjugate were determined from the NMR spectra of an alkali-treated product without hydrofluoric acid degradation. The structure was proved to consist of 1,3-linked poly(glycerophosphate) and a lipid anchor, Glc(α1-2)Glc(α1-3)acyl$_2$Gro, the former being linked to the 6-position of the distal glucose of the latter. Most of the 2-positions of the glycerol residues in the glycerophosphate part were substituted by oligoglucose esterified partially with alanine. The overall structure elucidated here thus coincides with the previous conclusion described by Fischer except for the linkage position of alanine. This result led us to conclude that the molecular species with this so-called LTA structure is not responsible for the IL-6 inducing activity. (Chapter III)

The structural analysis of one of the cytokine-inducing components was next performed. The component was similarly subjected to hydrofluoric acid hydrolysis. A major hydrophilic product was further subjected to acetolysis. The acetolysis products were separated and characterized by means of NMR and MS. By talking all the available information into account, the component was concluded to consist of a mannose rich highly branching polysaccharide and a modified poly(glycerophosphate) structure containing acyl groups, the former being linked to the later *via* phosphodiester linkage. (Chapter IV)

List of publications

Suda, Y., Hashimoto, M., Yasuoka, J-i., Okabe, E., Kusumoto, S., Takada, H., Hayashi, T., Tamura, T., and Kotani, S. (1996) Immuno-Stimulating Macromolecular Glycolipids from Bacterial Cell Surfaces. *Polymer Preprints*, **37**, 129-130.

Hashimoto, M., Yasuoka, J-i., Suda, Y., Takada, H., Yoshida, T., Kotani, S., and Kusumoto, S. (1997) Structural feature of the major but not cytokine-inducing molecular species of lipoteichoic acid. *J. Biochem.* **121**, 779-786.

Publications on other research subjects

Setsune, J-i. and Hashimoto, M., (1994) Synthesis and Separation of *meso*-tetraarylporphyrins with C_i Symmetry. *J. Chem. Soc., Chem. Commun.* 657-658.

Suda, Y., Hashimoto, M., Yasuoka, J-i., Kusumoto, S., Oku, N., Ding, J.L., and Ottenbrite, R.M., (1996) *Exo-vivo* Cytokine Inducing Activity of Hydrophobized Poly(maleic acid-*alt*-7,12-dioxaspiro-[5,6]-dodec-9-ene) [Poly(MA-CDA)]. *J. Bioactive Compatible Polymer*, **11**, 100-109.

Liu, w-c., Oikawa, M., Fukase, K., Suda, Y., Winarno, H., Mori, S., Hashimoto, M., and Kusumoto, S. (1997) Enzymatic preparation of (*S*)-3-hydroxytetradecanoic acid and synthesis of unnatural analogues of Lipid A containing the (*S*)-acid. *Bull. Chem. Soc. Jpn.*, **70**, in press.

Acknowledgement

The author would like to express his sincerest gratitude to Professor Shoichi Kusumoto for his instructive suggestions and valuable discussion throughout the work. The author is also grateful to Professor Sumihiro Hase and Professor Ikuo Ueda for their careful reading of this dissertation and invaluable advice.

The author is indebted to Dr. Yasuo Suda for his important suggestions and guidance during the work, Dr. Koichi Fukase and Dr. Masato Oikawa for their kind advice on various problems and encouragement.

The author is thankful to Dr. Jun-ichi Setsune for his great deal of effort at the beginning of the work.

The author wishes to thank to Professor emeritus Syozo Kotani for his helpful advice.

The author also thanks to Professor Haruhiko Takada at Tohoku University for his kind supply of a seed culture of *Enterococcus hirae* ATCC 9790, Professor Tadamitsu Kishimoto at Osaka University School of Medicine for his generous supply of rHuIL-6, and Professor Seiki Kuramitsu at Graduate School of Science, Osaka University and Professor Toshihide Tamura, Dr. Tomoko Hayashi, Ms. Kazue Aoyama, and all members at Department of bacteriology, Hyogo College of Medicine for the invaluable help including bacterial cells and biological tests.

Thanks are given to Dr. Kaoru Inami at Protein Research Foundation for amino acid analysis, Dr. Yasuhiro Itagaki, Dr. Hideo Naoki, and Ms. Miki Miyaji at Suntory Institute for Bioorganic Research for measurements of MALDI-TOF-MS, Dr. Keonil Lee, Mr. Seiji Adachi for their skillful measurements of NMR spectra, Mr. Hiroshi Adachi for measurements of mass spectra.

The author especially thanks to Jun-ichi Yasuoka, Yoshimasa Imamura, Eriko Okabe, and Yoshiyuki Fukase for their help in experiments and all members in Kusumoto laboratory for their fruitful discussion.

Finally, the support of my parents which enabled my study in doctor course at Osaka University is gratefully acknowledged.